9-1-2015

Investigation of Membrane Fouling and Cleaning in Direct Contact Membrane Distillation of Municipal Wastewater

Michelle Miller

Michelle D. Miller

Candidate

Civil Engineering

Department

This thesis is approved, and it is acceptable in quality and form for publication:

Approved by the Thesis Committee:

Kerry Howe , Chairperson

Bruce Thomson

Andew Schuler

Investigation of Membrane Fouling and Cleaning in Direct Contact Membrane Distillation of Municipal Wastewater

by

Michelle D. Miller

B.S., Civil Engineering, University of New Mexico, 2012

THESIS

Submitted in Partial Fulfillment of the

Requirements for the Degree of

Master of Science

Civil Engineering

The University of New Mexico

Albuquerque, New Mexico

July 2015

ACKNOWLEDGEMENTS

I would like to especially thank my advisor and committee chair, Dr. Kerry Howe, for all of the effort and time he invested for my research. Dr. Howe's dedication and knowledge has helped my project become a success and my future become brighter. My committee members, Dr. Bruce Thomson and Dr. Schuler, provided their time and contributed their knowledge to also to enhance the success of this project. I am appreciative to have been able to work with such a knowledgeable group.

Thank you to the CREST program at the National Science Foundation for their funding and support for this research. This project would not have been able to succeed otherwise.

Thank you to Jeff Romanowski and the operators at the Albuquerque Bernalillo County Water Utility Authority (ABCWUA) Southside Water Reclamation Plant (SWRP) who were very helpful and supportive for obtaining the municipal wastewater effluent samples used for this project.

Thank you to Mike Spilde at the Earth and Planetary Sciences department for the wonderful membrane SEM imagery.

I would also like to thank Mike Rupert at Rupert Pipe Fabricating for making custom heating and cooling coils.

Investigation of Membrane Fouling and Cleaning in Direct Contact Membrane Distillation of Municipal Wastewater

by

Michelle D. Miller

B.S., Civil Engineering, University of New Mexico, 2012

Master of Science

Civil Engineering

The University of New Mexico

Albuquerque, New Mexico

July 2015

Abstract

Municipal wastewater discharge to the environment is generally subject to regulations established under the Clean Water Act. Though the water is highly treated it is not suitable for human consumption. Increased interest in water reuse for potable supply introduces concern about trace constituents present in their water, such as pharmaceuticals and endocrine disruptors. Current treatment processes, such as reverse osmosis, are used to remove many of these compounds, but is expensive and energy intensive. The rise of interest in potable water reuse may cause consumers to be

concerned about trace constituents present in their water and would require additional treatment. Membrane distillation may be applicable in some circumstances to treat the effluent from municipal wastewater treatment plants with a low grade heat source for direct potable reuse. This project investigated the chemical cleaning efficiency of ethylenediaminetetraacetic acid (EDTA) on membrane wastewater effluent fouling for direct contact membrane distillation (DCMD) to help assist wastewater reuse become a reality.

A laboratory scale DCMD system was designed and constructed including a warm feed loop and cold permeate loop to utilize a flat sheet, crossflow membrane cell. Treated wastewater effluent collected from the Albuquerque Bernalillo County Water Utility Authority (ABCWUA) Southside Water Reclamation Plant (SWRP) was used as the feed solution. The performance of the MD system was tested and evaluated using parameters including flow rate, feed and permeate temperature, feed water quality, permeate flux, membrane area, cross flow velocity, and membrane type and pore size. An (EDTA) cleaning solution was used to clean a 0.2μm polypropylene (PP) membrane that had reached a 50% flux decline due to wastewater effluent fouling. The cleaning process was repeated on the membrane three times to determine the effectiveness of removing wastewater effluent fouling by permeate flux recovery.

Overall system data collection and analysis determined the influences of system parameters on permeate flux, constituent rejection, membrane fouling rate, and a membrane chemical cleaning. Results produced from this study give a better

understanding of the membrane distillation process, and membrane cleaning when treating municipal wastewater effluent, and gives potential to DCMD for becoming an optional process for potable water reuse.

Table of Contents

Chapter 1: Introduction

1.1 Problem Statement

Water is essential for all life forms and sustains their existence on Earth. Water is a limited resource, and potable water for human consumption is increasingly scarce. Many communities in New Mexico face a challenge for sustaining a consistent reliable water source since it is a desert and experiences many droughts. Albuquerque is located in the central part of New Mexico and uses both groundwater and surface water for its water supply.

It was realized in the 1990's that the aquifer which supplies Albuquerque had been shrinking at an unsustainable rate. In 2008 the San Juan Chama Drinking Water Project was completed to enable the city to take full advantage of its surface water supplies. As a consequence, water levels in the aquifer have risen by 10 to 20 feet beneath most of the city. The aquifer water table depths in two Albuquerque areas from 1998 to 2013 from the U.S. Geological Survey are shown in Figure 1.1.

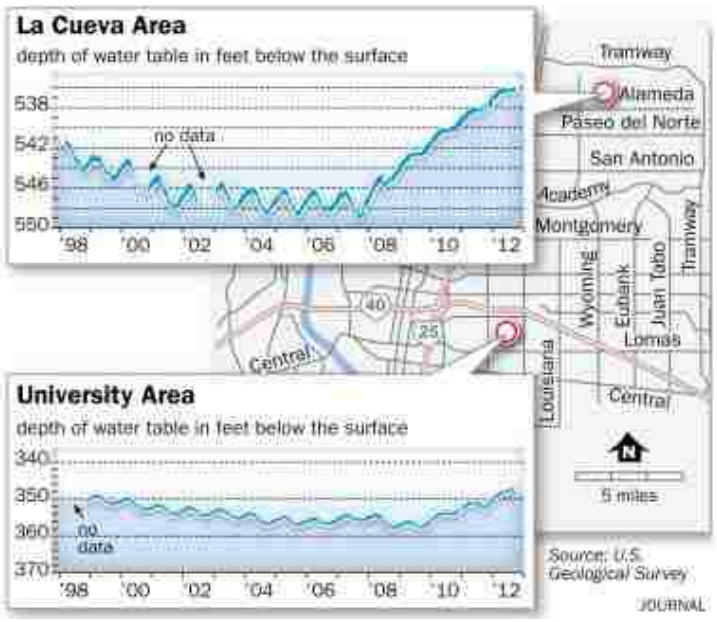

Figure 1.1 Aquifer rising despite drought by John Fleck, Albuquerque Journal October 8, 2013. http://www.abqjournal.com/276444/news/aquifer-under-city-still-rising-despite-drought.html

Recharge is due to infiltration of runoff along the mountain front, and groundwater infiltration along the Rio Grande. Even with the diversion project completed and functional, the aquifer is still drawn upon at an inconsistent rate. Yearly droughts require the city to reduce surface water diversion and in turn rely on the overtaxed groundwater source. In other communities where groundwater pumping was not reduced, such as Rio Rancho, the aquifer table continues to decline. Therefore, Albuquerque's water sources for drinking and municipal supply consist of a blend of limited surface water from the river and unsustainable groundwater.

The surface water from the river is treated at the San Juan-Chama Water Project Surface Water Treatment Plant located north of the wastewater treatment plant. Used water from the city is collected and treated to current acceptable standards at the Southside

Wastewater Reclamation Plant, where the effluent is released into the Rio Grande. The treated wastewater outfall flows into the environment and downstream to Texas and Mexico, where multiple ecosystems exist along the way. The wastewater plant does not treat the wastewater to potable criteria and therefore pollutants are being discharged into the surface water and the environment. Along with naturally occurring groundwater and surface water contaminants, the presence of contaminants of emerging concern (CEC's) such as pharmaceuticals and personal care products (PPCP's) and endocrine disruptor chemicals (EDC's) are becoming of interest to the public. These trace organic compounds have been found in the world's wastewater effluent, surface water, groundwater, and drinking water since 2000 (WHOrganization 2011), including Albuquerque's wastewater and surface water treatment plant's influent and effluent, and groundwater pump stations (ABCWUA 2011). Unfortunately, current municipal wastewater purification techniques do not treat wastewater to drinking water quality. Current water treatment techniques are energy extensive resulting in a higher operational cost with recurrent material repair and replacement. Membrane distillation has shown potential to overcome these water treatment disadvantages, while completely removing all non-volatile constituents (Alkhudhiri et al. 2012, Susanto 2011, El-Bourawi et al 2006, Tomaszewska 2000, Lawson and Lloyd 1997).

1.2 Membrane Distillation Background

Membrane distillation (MD) is a thermal distillation process which uses a hydrophobic membrane and involves three core steps: evaporation, vapor transport, and condensation. The four main MD configurations (shown in Figure 1.2) are air gap membrane distillation

(AGMD), sweeping gas membrane distillation (SGMD), vacuum membrane distillation (VMD), and direct contact membrane distillation (DCMD). AGMD requires a warm liquid feed solution to be in contact with the membrane with a stagnant air gap in between the opposing side of the membrane and a cool condensation surface. SGMD has a similar set up as the AGMD, but the air gap is composed of a cold inert gas that sweeps the vapor to a condenser outside the membrane module. DCMD involves a warm feed liquid solution and a cool liquid permeate solution that are both in direct contact with the membrane and allows water vapor to transfer from one solution to the other. VMD has a similar set up as DCMD, but with a vacuum on the permeate side to drive the vapor across and to a condenser outside of the module.

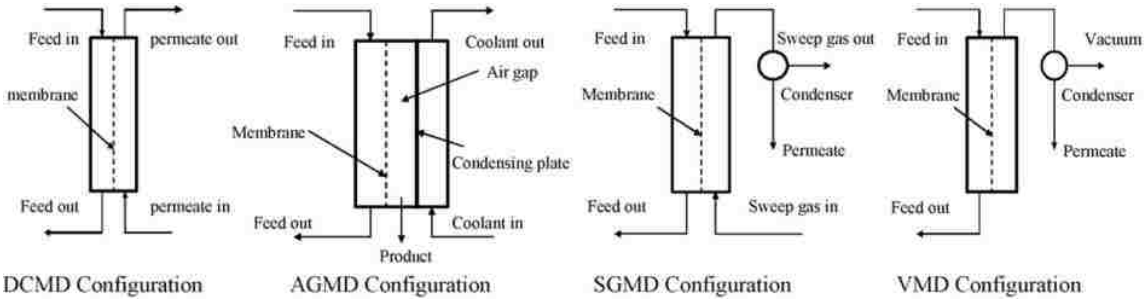

Figure 1.2 The four main MD configurations. (El-Bourawi et al 2006)

In DCMD the contact of the liquid feed and the liquid permeate with the membrane results in a liquid/vapor interface that is formed at the pore entrances on both sides. Liquid surface tension maintains a vapor phase inside the membrane pores, which keeps the feed and permeate liquids out. Molecules of volatile components, such as water, present in the feed solution evaporate as they cross the feed liquid/vapor interface,

migrate across the pore vapor space, and condense back into a liquid as it passes through the permeate vapor/liquid interface. A temperature differential of at least 10°C across the membrane pores provides the energy for the phase change. The driving force of the vapor movement is due to the transmembrane vapor pressure differential between the feed and permeate side of the membrane, which is caused by this temperature difference. MD does not rely on pressure for filtration nor does the feed solution have to reach boiling point in order to evaporate volatile molecules. The evaporation process only requires a latent heat of vaporization from a 30-90°C heat source to achieve the characteristic phase change from liquid to vapor. A low operational heat requirement makes the process suitable for utilizing low or waste grade heat sources.

Wastewater effluent cause filtration membrane pores to foul, causing a reduction in clean water production. In DCMD, pore fouling can lead to pore wetting which can allow dissolved constituents in the feed water to pass through the membrane. There are four main types of wastewater fouling: particulate fouling, inorganic scaling, organic fouling, and biofouling or microbial fouling. Particulate fouling is caused by suspended solids, colloids, and biologically inert particles which accumulate on the surface and block the membrane pores. Scaling is due to constituent accumulation of precipitates on the membrane surface such as metal oxides, inorganic colloids, calcium sulfate, carbonate, fluoride, barium sulfate, and silica. Constituents responsible for biological and microbial fouling include bacteria, microorganisms, and can cause concentration polarization. Organic fouling is caused by natural organic matter (NOM). Fouling associated with MD of wastewater likely includes pore narrowing, cake formation, pore plugging can cause

membrane pore wetting or blockage. These fouling mechanisms can cause undesirable effects such as decline in permeate flux or decreased permeate qualify through the membrane. Since membrane fouling adversely effects all membrane processes including MD, further research in this category is necessary to advance the separation process.

1.3 Research Objectives

The purpose of this research was to investigate the mechanisms of membrane wastewater effluent fouling for a laboratory scale DCMD system. System functionality, system parameters, and membrane fouling mechanisms due to treated municipal wastewater and its removal were evaluated. Application of an ethylenediaminetetraacetic acid (EDTA) chemical cleaning process was explored to gain insight to potential membrane permanence for DCMD wastewater reuse applications.

Objectives

The main objective of this research was to conduct scientific laboratory scale DCMD experiments to verify if a cleaning solution could effectively recover permeate flux from treated wastewater constituent membrane fouling. The effect of using a wastewater feed in DCMD on membrane flux was determined. The type of fouling on DCMD membranes used to treat wastewater was characterized. The ability to restore DCMD performance by membrane cleaning with EDTA was determined. In addition, further understanding of DCMD and its effectiveness and requirements for wastewater reuse applications was obtained. The process advantages associated with RO, such as a high permeate flux, are going to attempted to be matched, while also overcoming the current disadvantages of

high operational pressure. Previous studies investigating RO membrane cleaning gave guidance of chemical, dose, pH level, crossflow velocity, temperature, and time for membrane cleaning to use for the wastewater effluent fouled MD membranes. Investigating these parameters and results for DCMD will help to gain a better understanding of the process for treating wastewater effluent to help further the implementation of industrial production of water reuse. This laboratory scale system was intended to assist in evaluating the effectiveness of using DCMD for wastewater reuse and to identify potential issues that must be addressed to further develop the technology. Additional research must be conducted for furthering the subject in large scale production, commercialization, sustainability and cost effectiveness. In order to address these objectives, the following tasks were completed.

Task 1: Construct a laboratory-scale DCMD system with main components shown in Figure 1.3. This task included a hydraulic test to check for and eliminate leaks, instrument calibration, and accurate data collection verification.

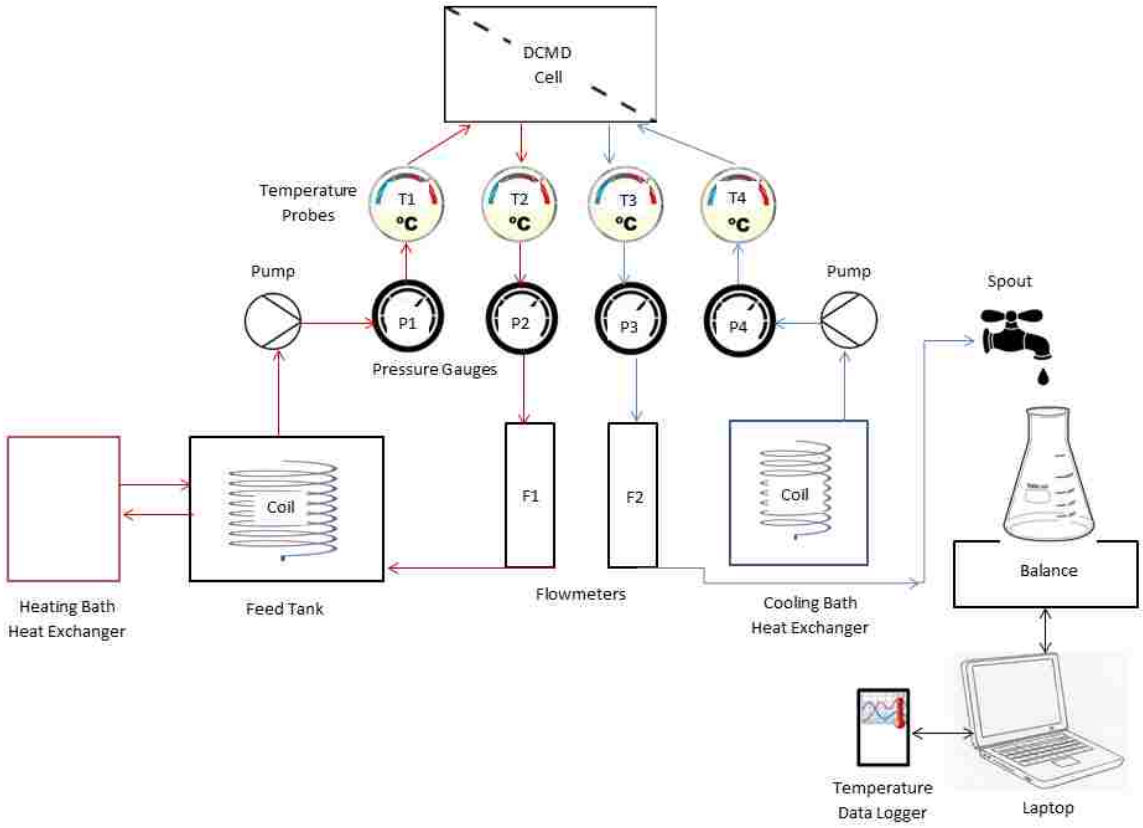

Figure 1.3 Process flow diagram for laboratory scale DCMD system

Task 2: Evaluate the performance of the DCMD system relative to similar systems in peer-reviewed literature.

Task 3: Investigate fouling of DCMD membranes by treated wastewater.

Task 4: Investigate the effect of a chemical cleaning process on the DCMD membrane fouling by comparing initial, declined, post cleaning system flux, and permeate conductivity, and pH.

1.4 Thesis Organization

With current potable water issues on the rise, wastewater reuse has become a sustainable option for regions such as Albuquerque, New Mexico. MD has the potential to be used in

wastewater reuse applications with further examination to the technology. The remaining of this paper goes into greater detail of how this DCMD research was performed along with laboratory testing results and conclusions. Chapter 2 discusses the background and literature reviews on MD, PPCP's and EDC's and the current treatment processes that are available to attempt to remove them, and chemical membrane cleaning. Chapter 3 covers the experimental methods that were used to acquire accurate data. Chapter 4 covers the results from the various laboratory experiments. Finally, Chapter 5 concludes the results and gives recommendations for possible future studies related to DCMD for water reuse applications.

Chapter 2: Background and Literature Review

This chapter covers backgrounds for the topics of interest that are related to this research. The history and background of membrane distillation is followed by the advantages of the process. A background on a few CECs is given followed by the information on current water treatment processes that remove them. The most familiar membrane treatment process for removal of dissolved constituents is reverse osmosis (RO). RO is discussed further to consider some of its disadvantages with regards to constituent removal. Studies on RO membrane cleanings that used a similar system set up as this DCMD research project are discussed.

2.1 History of Membrane Distillation

Membrane distillation was first patented in 1963 by Bruce Bodell for water desalination with the use of a silicon rubber membrane (Lawson and Lloyd 1997). In 1964, RO gained more recognition because of its ability to produce a relatively higher permeate flux of 20-75 L/ m^2h (while DCMD reported up to 1 L/ m^2h) for desalination and the industry's lack of interest to invest in any other new processes (El-Bourawi et al. 2006) (Lawson and Lloyd 1997). Current typical RO fluxes are 1-75 L/m^2h (.6-30 gal/ft^2d) and similarly 1-75 L/ m^2h for MD (Alkhundhiri 2012). MD was reconsidered as a comparable separation process to RO when new and improved membranes and model designs became available in the 1980's to allow higher MD flux development (Lawson and Lloyd 1997, Tomaszewska 2000, El-Bourawi et al. 2006).

Membrane porosities as high as 80% and thicknesses as low as 50 micrometers(μm) were designed, which allowed for a 100 times greater production efficiency compared to the results from the 1960's (Lawson and Lloyd 1997). Production efficiency is defined by the ratio of the heat required for vaporization to the total amount of heat including the vaporization heat, heat loss through the membrane and pores, and heat loss from liquid bulk temperatures to the temperature at the membrane surfaces. In contrast to RO, MD has yet to be implemented by the wastewater treatment industry (El-Bourawi et al. 2006). However, MD has been successfully evaluated in many laboratory scale applications (El Bourawi et al. 2006, Tomaszewska 2000, Lawson and Lloyd 1997, Susanto 2011, Koschikowski 2008). MD has gained a lot of attention and interest since better suited materials, models, and more knowledge about the process have emerged (Khayet 2011). The process may find application where there are large sources of low grade or waste heat, low pressure, all while providing potential solutions for current and future water demands.

MD configurations have been considered for desalination, but also for other water purifications applications such as nuclear, textile, chemical, pharmaceutical, wastewater, and food industries (Lawson and Lloyd 1997, El-Bourawi et al. 2006). MD has been shown to be effective for both distilled water production and concentration of aqueous solutions (El-Bourawi et al. 2006). Out of the four MD configurations, DCMD has been shown to be suited for applications for which the permeate is mostly water and when non-volatile solution contaminants are present (El Bourawi et al. 2006, Lawson and Lloyd 1997).

2.2 Advantages of Membrane Distillation

Many advantages and benefits accompany MD from a water treatment perspective. Since the process is thermally driven, the transmembrane hydrostatic pressure required ranges from 0-29 psi (0-2 bar). In comparison, RO requires from 73-1200 psi (5-85 bar) (Howe et al. 2012). The pressure that RO requires is generated by pumps which use electricity. Electricity is a costly high-grade form of energy and depletes natural resources. Feed temperatures for MD range from 30-90°C which can be generated from low grade waste heat or alternative heat sources such as geothermal or solar panels (Lawson and Lloyd 1997, Tomaszewska 2000, El-Bourawi et al. 2006, Gryta et al. 2006). Vacuum distillation can also use low grade heat, but has more complexity than MD. Conversely, conventional thermal distillation needs the liquid to reach its boiling point, requiring heat above 100°C. This heat requirement is more expensive to generate and is more difficult to generate with alternative heat sources. It is speculated that low operational pressure and temperature for MD lessens the physical wear on the membranes which decreases compaction of the fibers significantly, reducing repair and replacement frequency. Compared to conventional distillation, the thinness of the membrane reduces vapor travel distance in the membrane pores, which allows for higher vapor water flux. Since the water vapor molecules have a shorter distance to travel across within the membrane matrix, less heat is transferred to the membrane matrix and through the membrane pore vapor space.

Another advantage of MD is that it is not limited by the non-volatile solute concentration of the aqueous feed solution since it is driven by temperature differentials (El-Bourawi et

al. 2006). Since RO is pressure driven to exceed the osmotic pressure gradient caused by the concentration gradient between the water in the permeate and in the solute concentrated feed solution, the feed concentration limits the process. The higher the concentration (or ionic strength) is in RO, the more pressure is required to maintain the permeate flux, and the constituent rejection is lessened (Howe et al 2012). With regards to waste streams, MD has the capability of recovering effluent in crystal form, if solid salvage was desired for disposal or reuse (El-Bourawi et al. 2006). RO has a typical recovery of 80 to 90% for colored or brackish groundwater and 50% for seawater (Lee et al. 2012). Another attractive aspect of MD is that theoretically 100% of ions, macromolecules, colloids, cells, and other non-volatile constituents are rejected. Processes such as RO, UF, and MF have not been able to claim such results (Lawson and Lloyd 1997). The MD system does not require high pressurized equipment compared to other separation processes such as RO. Lawson and Lloyd claimed that MD is a more efficient process than RO for removing ionic compounds and non-volatile organic compounds from water. This removal efficiency also applies to the CEC's, which are gaining more recognition since they can cause adverse health effects for humans, animals and ecosystems. Once implemented in large scale, MD could give water treatment plants a reliable process to apply to their treatment trains to remove these contaminants along with the other regulated contaminants.

2.3 Personal Care Products and Pharmaceuticals and Endocrine Disrupting Chemicals

CEC's consist of chemicals that are becoming discovered in water that previously had not been detected or are being detected at levels that were not expected (EPA 2014). PPCPs and EDCs fall within this category. Pharmaceuticals are synthetic or natural chemicals found in prescription medications, over the counter drugs, and veterinary drugs. Personal care products include items such as lotions, creams, soaps, and hair products etc. EDCs are natural or synthetic chemicals that have an adverse effect on the body's endocrine system with possible developmental, reproductive, neurological and immune impacts. These thousands of compounds contain active ingredients and are introduced into the environment via human and animal excretion, bathing, sewage effluent, improper medicine disposal, agriculture runoff, wastewater effluent, treated sludge, industrial waste, medical waste from healthcare and vets, and landfill leachate.

The presence of PPCPs and EDCs in water supplies has been known for many years, dating back to around the 1980's (WQA 2013). The original concern was associated with reports of physiological abnormalities associated with fish and other aquatic organisms in areas near or surrounding discharge sites of waste water treatment facilities. Over time the contaminant concerns associated with waste water effluent have expanded into the field of drinking water. These contaminants are found in water as multiple organic and inorganic forms. Granted, the detection of them is considerably low, typically reported from 0.05 μg/L to 0.1 μg/L, but the potential effect of these compounds and metabolites at this concentration on biological organisms are unknown (WHO 2011, WQA 2013).

Despite the low the detection of these contaminants, PPCPs such as polybrominated diphenyl ethers (PBDEs) and perflourinated compounds (PFCs) accumulate in human tissue or blood and are associated with health effects including endocrine disruption (EPA 2013). The World Health Organization (WHO) stated that advanced and costly water treatment technology (including RO) will not be able to completely remove all pharmaceuticals to concentrations less than the detection limits of the most sensitive analytical procedures at all times. Under proper operation, MD has the potential to overcome this problem with its ability to selectively filter out pure water from its feed source using temperature as its driving force. Membranes from MD can be in charge of filtering out and CEC's rather than accumulating in the body of the consumer.

2.4 Current Processes and their Removal of PPCPs and EDCs

Currently, there are options for wastewater treatment plants to remove the traditional regulated constituents and PPCPs and EDCs. The four processes available are biological treatment with activated sludge and membrane bioreactors, reverse osmosis (RO), activated carbon adsorption, and advanced oxidation. Conventional wastewater treatment facilities commonly have activated sludge processes or other forms of biological treatment. These processes have revealed varying removal rates for pharmaceuticals, ranging from less than 20% to greater than 90% (WHO 2011). The efficiency of these processes for the removal of pharmaceuticals varies between studies and is dependent on each operational configuration of the wastewater treatment facility. Biological wastewater treatment, especially membrane bioreactors, provide high quality feed water for succeeding processes, but are not effective at removing all micro constituents. Some

chemicals have shown complete or partial resistance to removal. For example, a biological wastewater treatment study showed that out of 49 PPCP compounds, seven of them had 0% removal and two thirds of the compound list only had 50% removal (Lee et al. 2009).

Out of the four current processes mentioned that can be used for water contaminant removal, RO appears to be the most dependable and promising logistically compared to the other three, though it is not 100% reliable. RO is a pressure driven membrane separation process in which dissolved constituents are separated from a solution by preferential diffusion as the solvent and solute molecules pass through a permeable material (Lee et al. 2012). The system uses a membrane with pore sizes of 0-.001μm with typical transmembrane pressure of 73-1200 psi (Howe et al. 2012). RO effectively removes particles, sediment, algae, protozoa, bacteria, small colloids, viruses, dissolved organic matter, 80-99% of divalent ions, and 80-99% (with nonporous membranes) of monovalent species (Lee et al. 2012, Howe et al. 2012). The RO process also effectively removes dissolved solutes except for volatile species. Many advantages originate with RO including a high flux, high constituent percentage removal, and in some cases high recovery. Though RO has multiple advantages associated with it, MD could potentially deliver the same advantages while surpassing RO's limiting disadvantages.

2.5 Comparison of Reverse Osmosis and Membrane Distillation

MD and RO both have a disadvantage involving scaling and fouling of the membrane. Scaling and fouling are due to particulate matter, precipitation of inorganic salts,

oxidation of soluble metals, and biological matter (Lee et al. 2012). Membrane scaling and fouling will cause permeate flux decline due to cake formation and pore blockage, and allow contaminants to breach the membrane due to pore wetting. Cleaning processes have been investigated primarily for RO membranes. Both processes are not very effective in removing volatile contaminants such as dissolved hydrogen sulfide (H_2S), dissolved carbon dioxide (CO_2), ammonia (NH_3), low molecular weight organics with low molecular weight, and solvents. However, if either is implemented at the end of an activated sludge treatment train, the aeration basins could remove these to make sure they are not in the feed solution for the RO or MD process.

Both processes are subject to concentration and temperature polarization. Temperature polarization is shown in Figure 2.1. Delta (δ) represents the thickness of the feed and permeate temperature boundary layers (*ft* and *pt)*, feed concentration boundary layer (*fc)*, and membrane (*m)*. Temperature (*T)* represents the temperature of the feed bulk solution (*fb)*, at the membrane surface on the feed side *(fm)*, at the membranes surface on the permeate side *(pm)*, and of the permeate bulk solution *(pb)*.

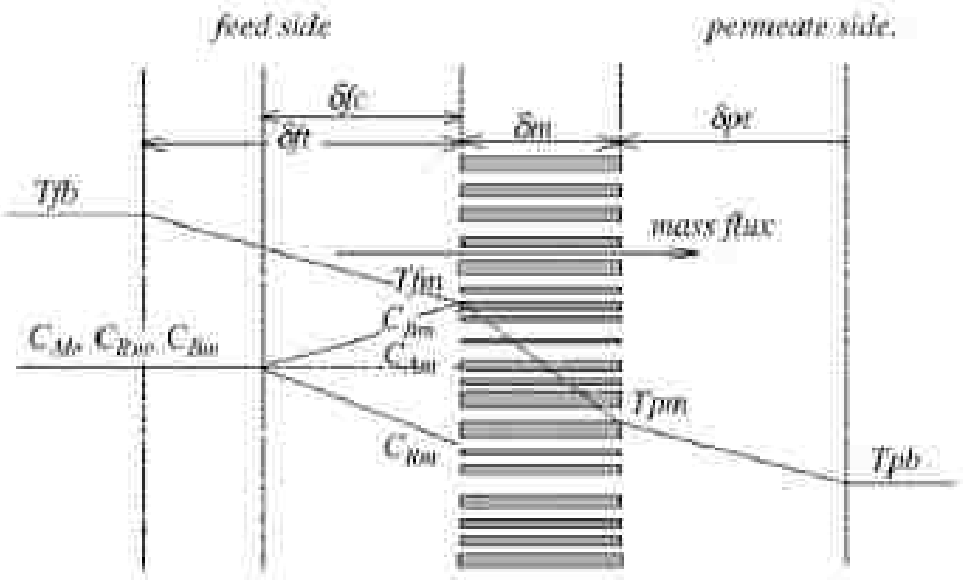

Figure 2.1 Temperature and concentration polarization in MD. (El-Bourawi et al. 2006)

Reverse osmosis rejects constituents based on size, polarity, and charge. Because of this, it removes a lot of contaminants well, but has some exceptions. Examples of what it does not remove so well besides volatile contaminants include small uncharged molecules, small polar molecules, neural acids and bases, and boron and silica in their neutral forms (Howe et al. 2012). Other disadvantages involve incomplete removal of PPCPs, EDCs, and molecules with similar physical and chemical properties. N-Nitrosodimethylamine (NDMA), which is a member of an extremely potent carcinogen family, has been shown to have poor removal by RO with varying removal ranges of 0-86% (Plumlee 2008, Steinle-Darling et al. 2007, Fojioka et al. 2012). Although ultraviolet (UV) treatment can effectively remove NDMA, there is considerable interest in the development of less expensive alternative treatment technologies (Mitch et al 2004). Like PPCPs and EDCs, neutral and hydrophobic compounds such as caffeine and Biphenyl-A (BPA) had less

than 50% removal by RO (Lee et al. 2009). Since these contaminants are non-volatile, MD should reject them without difficulty.

As any other separation process, there are some barriers to MD to be addressed. The barriers include module design for heat loss especially for DCMD, resulting in high thermal energy consumption and uncertain cost and energy estimates (El-Bourawi et al. 2006). The mass transport process also appears to be more complex and produces a lower flux compared to pressure driven processes. Despite the potential drawbacks, if an MD system is functional and implemented correctly, they can be minimized or surpassed while achieving fluxes comparable, if not better than RO with potentially complete non-volatile constituent removal.

2.6 Microporous Membrane Chemical Cleaning

Many studies have been performed evaluating chemical and physical cleaning of membranes, but mainly for RO systems (Ang et al. 2011, Ang et al. 2006, Madaeni and Samieirad 2010). A particular study examined the protein fouling, the role of hydrodynamic conditions, feed solution chemistry, and membrane properties for RO, nanofiltration (NF), and ultrafiltration (UF) membranes (Wang and Tang 2011). They found that the membranes with smoother, more hydrophilic, and electrostatic repulsive surfaces experienced less initial fouling, but at the end of 4-day testing showed that flux had little dependence on membrane properties. They concluded that long term fluxes are controlled by foulant-fouled membrane surface's interaction with the feed solution. Another study by Madaeni and Samieirad used a RO hydrophilic polyamide membrane for treatment of industrial wastewater. The membrane was fouled with organics for 540

minutes and then cleaned with various chemical solutions in attempt to dissolve the membrane surface deposits. Results showed that acids were not effective in recovering flux, but that introducing an acid after a caustic and detergent cleaning was effective (Madaeni and Semieirad 2010). They noted that effective cleaning chemicals should loosen and dissolve foulants, keep them in dispersed solution form, avoid new fouling, and not attack the membrane.

Research on membrane cleaning was conducted by a group at Yale University between 2006 and 2011. All studies were performed with a laboratory scale crossflow unit test consisting of a rectangular plate and frame cell and channel, flat sheet thin film composite LFC-1 model RO membrane, pumps, feed reservoir, temperature control system and a data acquisition system. The first test by Ang, Lee, Chen, and Elimelech in 2006 used alginate and natural organic matter to simulate effluent organic matter fouling on the membrane and an alkaline solution, metal chelating agent, and anionic surfactant were used as chemical cleaning agents. They found that cleaning agent type and combination, cleaning solution pH, cleaning agent dose, cleaning time, and channel crossflow velocity vary the cleaning effectiveness of fouling. In addition, they noted that the fouling layer composition influences the reactivity of cleaning agent with organic and non-organic foulants. They concluded that sodium hydroxide (NaOH) alone gave poor cleaning results, but (EDTA) and sodium dodecyl sulfate (SDS) alone were quite effective.

The second study was by Ang, Tiraferri, Chen, and Elimelech in 2011 and focused on fouling and cleaning of the same RO model membrane and set up, but using mixtures of organic foulants to simulate wastewater effluent. The foulants included alginate, bovine serum albumin, Suwannee River NOM, octanoic acid, and calcium ions. The cleaning agents studied were an alkaline solution, metal chelating agent, anionic surgactant, and a concentrated salt solution. The cleaning experiments also showed that NaOH alone was not effective in disrupting organic foulants, mainly calcium. They gave evidence that found sodium chloride (NaCl), SDS, and EDTA to be effective at cleaning foulants, especially if applied at high pH and for longer cleaning times of 15 minutes.

The third study by Ang, Yip, Tiraferri, and Elimelech in 2011 studied actual wastewater effluent fouling on the same RO model system and investigated singular and dual step cleaning processes. The effluent was from a municipal wastewater treatment plant in Connecticut. The chemical cleaning agents used for first and second stage cleaning were DI water, NaOH, NaCl, SDS, and EDTA. They demonstrated that strategically pairing chemical agents can have a higher cleaning efficiency for the effluent fouled layer such as NaOH and NaCl and the mismatching of chemical agents such as EDTA with SDS can result in a dramatic decrease of cleaning performance. Single stage 15 minute cleaning times demonstrated to have the highest cleaning efficiencies especially chemicals EDTA and SDS. The results of these studies have been relied upon for determining the cleaning agents to be used for the DCMD experiments since their set ups were very similar and the feed solutions were also comparable to a certain degree.

Chapter 3: Experimental Methods

3.1 Experimental Methods Overview

A laboratory scale system consisted of direct contact membrane distillation cell, a hot closed feed loop, and a cold permeate loop. The hot closed loop included a heating bath heat exchanger, feed solution tank, and a pump. The cold loop included a cooling bath heat exchanger, pump, and a permeate collection flask positioned on an analytical balance. Temperature probes, pressure gauges, and flowmeters were installed at the inlet and outlet of the membrane cell. The temperature data was collected using an Omega 4 channel data logger from McMaster Carr. The balance and the temperature data logger were connected to a laptop for automatic data collection of system temperatures and permeate flowrates. The process flow diagram for the system is shown in Figure 3.1. The DCMD system was used to investigate three phases of system operation properties. The first phase involved saline and wastewater effluent feed solutions using three flat sheet membranes to gather system parameter effects on permeate flux. The second phase included membrane fouling properties of treated wastewater on two membranes. Phase three investigated a chemical cleaning efficiency for permeate flux recovery for one of the three membranes. Details of the phase testing are discussed in the remainder of the chapter, and can be seen in the experiment matrixes found in Tables 3.1, 3.2 and 3.3.

Table 3.1 NaCl Feed Solution Experiment Matrix

NaCl Tests	Parameter Variable	Feed In (T1) (°C)	Permeate Out (T3) (°C)	ΔT (°C)	Crossflow (m/s)	Membrane	Membrane Pore Size
1	BASELINE	40	20	20	0.24	Laminated PTFE*	0.22µm
2	Feed Temperature	50	30	20	0.24	Laminated PTFE	0.22µm
3	Feed Temperature	60	40	20	0.24	Laminated PTFE*	0.22µm
4	Feed Temperature	70	50	20	0.24	Laminated PTFE*	0.22µm
5	Delta T	50	20	30	0.24	Laminated PTFE	0.22µm
6	Delta T	45	20	15	0.24	Laminated PTFE	0.22µm
7	Cross-flow	40	20	20	0.29	Laminated PTFE*	0.22µm
8	Cross-flow	40	20	20	0.39	Laminated PTFE	0.22µm
9	Membrane&Feed T	40	20	20	0.24	PP*	0.2 µm
10	Membrane&Feed T	50	30	20	0.24	PP	0.2 µm
11	Membrane&Feed T	60	40	20	0.24	PP	0.2 µm
12	Membrane&Feed T	70	50	20	0.24	PP*	0.2 µm
13	Membrane&Feed T	40	20	20	0.24	PP	0.1 µm
14	Membrane&Feed T	50	30	20	0.24	PP	0.1 µm
15	Membrane&Feed T	60	40	20	0.24	PP	0.1 µm
16	Membrane&Feed T	70	50	20	0.24	PP*	0.1 µm

**indicates a new membrane was used at the beginning of the test.*

Table 3.2 Wastewater Effluent Feed Solution Experiment Matrix

WW tests	Parameter Variable	Feed In (T1) (°C)	Permeate Out (T3) (°C)	ΔT (°C)	Crossflow (m/s)	Membrane	Membrane Pore Size
1	Feed Temperature	40	20	20	0.24	Laminated PTFE	0.22µm
2	Feed Temperature	60	40	20	0.24	Laminated PTFE	0.22µm
3	Delta T	60	20	40	0.24	Laminated PTFE*	0.22µm
4	Cross-flow	40	20	20	0.39	Laminated PTFE	0.22µm
5	Feed Temperature	40	20	20	0.24	PP	0.1µm
6	OVERNIGHT	40	20	20	0.24	PP	0.1µm
7	Cross-flow	40	20	20	0.29	PP	0.1µm
8	OVERNIGHT	40	20	20	0.24	PP	0.1µm

**indicates a new membrane was used at the beginning of the test.*

Table 3.3 EDTA Membrane Cleaning Experiment Matrix

Membrane Cleaning	Feed Solution	Feed In (T1) (°C)	Permeate Out (T3) (°C)	ΔT (°C)	Crossflow (m/s)	Membrane	Membrane Pore Size	Cleaning Time
1	WW Effluent	70	50	20	0.15	PP*	0.2µm	
1	2mM EDTA pH 11	70	-	-	0.15	PP	0.2µm	15 min
1	WW Effluent	70	50	20	0.15	PP	0.2µm	
2	WW Effluent 1	70	50	20	0.13	PP*	0.2µm	
2	2mM EDTA pH 11	25	-	-	0.13	PP	0.2µm	30 min
2	WW Effluent 2	70	50	20	0.13	PP	0.2µm	
2	2mM EDTA pH 11	25	-	-	0.13	PP	0.2µm	30 min
2	WW Effluent 3	70	50	20	0.13	PP	0.2µm	
2	2mM EDTA pH 11	25	-	-	0.13	PP	0.2µm	30 min
2	WW Effluent 4	70	50	20	0.13	PP	0.2µm	

**indicates a new membrane was used at the beginning of the test.*

Phase One

The system properties and functionality were investigated by using a 500 mg/L NaCl feed solution, DI water permeate solution, and examined the permeate flux behavior of polytetrafluoroethylene (PTFE, also known as Teflon) 0.22μ, PP 0.2μ, and PP 0.1μ membrane in the first 16 tests seen in Table 3.1. The feed temperature, solution temperature difference between the feed and permeate sides of the membrane (delta T), channel cross-flow velocity, membrane type and pore size were all investigated to determine their effects on the permeate flux and process efficiency. The feed tank was filled with 10L of the NaCl solution and then heated to the appropriate feed temperature for each specific test. The permeate loop was filled with DI water and heated or cooled to the appropriate permeate temperature as well. Both loops were circulated and once a permeate flux was observed, Winwedge and the temperature data logger were activated to record the flux rate and temperature respectively. Each of the16 NaCl tests was run for approximately 1 hour each. The flowrates and pressures within the hot and cold loops were manually recorded. The temperature and permeate flux were automatically recorded into the data logger memory and into Excel via the Winwedge software respectively. Samples of the feed solution, DI water solution, and permeate solutions were collected at the beginning and end of each test to test pH and conductivity. All three virgin membranes were imaged using a Scanning Electron Microscope (SEM) to examine their surfaces and material structure.

Phase Two

Membrane fouling was investigated as a function of system performance and permeate flux. Wastewater effluent collected from the Southside Wastewater Reclamation Plant outfall was used for the feed solution. The 0.22 μm PTFE and 0.1 μm PP membranes were examined during this test. Feed temperature, delta T, channel cross-flow velocity, membrane type and pore size, and running time were evaluated to determine their effect on permeate flux behavior. The process of filling and controlling temperature of the feed and permeate loops as well as data collection procedures were the same as from phase one. Referring to the experiment matrix found in Table 3.2, tests 1-5 and 7 were run for approximately 1 hour. Tests 6 and 8 were run for approximately 27 and 41 hours respectively. SEM images and x-ray powder diffraction (XRD) results, shown in Chapter 5, of the fouled membrane surfaces and cross-sections gave a closer look at sources of membrane function disruption.

Phase Three

Phase three investigated the membrane chemical cleaning process efficiency of an EDTA solution on a wastewater effluent fouled 0.2μm PP membrane. Since membrane fouling is reduced when operating at a low feed temperature and a high cross-flow velocity, the wastewater feed solution was run at a high temperature with reduced channel crossflow velocities to allow for more rapid membrane fouling in this phase. Accelerated membrane fouling allowed for testing repeatability. A preliminary membrane cleaning test involved heating the wastewater effluent feed solution to 70 °C and the DI water permeate solution to 50°C, with both loops running at a cross-flow velocity of 0.15 m/s. The initial

permeate flux was determined by averaging fluxes from the first 90 minutes. The system ran until the permeate flux decline by approximately 50%. The feed loop was flushed with DI water (2-3 L) at room temperature with a cross-flow velocity of 0.15 m/s to discard the wastewater effluent. Next, a 0.002 M EDTA solution with a pH of 11 was heated to 70°C and circulated within the feed loop at a cross-flow velocity of 0.15 m/s for 15 minutes. Then 2-3 L of DI water was run through the feed loop again to flush out the cleaning solution. Fresh wastewater effluent was fed into the system again as before at 70°C with a cross-flow velocity of 0.15 m/s to establish a post cleaning flux in order to observe flux recovery. The Tygon tubing became slightly cloudy after running the 70°C EDTA solution, and the permeate samples conductivity were reported to be higher than expected.

Following the initial membrane chemical cleaning test, a series of cleaning tests as described above on one 0.2 μm PP membrane was completed. Tests involved cycling feed solutions of wastewater effluent, DI water, and then EDTA and are shown in Table 3.3. To help understand the cleaning effectiveness of the EDTA and membrane longevity, the membrane fouling and chemical cleaning procedure was repeated on the same membrane until a process failure was indicated. To begin the test, a 10L feed solution of wastewater effluent heated to 70°C and a DI water permeate solution at 50°C both ran at a 0.125 m/s cross-flow velocity. The system ran continuously until the permeate flux decline by about 55%. DI (2-3L) water at room temperature was used to flush the feed loop at 0.125 m/s and collected into a bucket. Next, 2mM EDTA with a pH of 11 at 26°C was circulated in the feed loop for 30 minutes. 2-3L of DI water was again run through

the feed loop to discard the cleaning solution. 10L of fresh wastewater effluent at 70°C with a cross-flow velocity of 0.13 m/s was used as the feed solution and the system was run continuously until the permeate flux declined to the previous value of about 55% of the initial flux. The initial and post cleaning fluxes were determined by averaging the first 90 minutes of the permeate flow rates. Samples of the feed solution were collected at the beginning and end of the wastewater effluent fed tests to measure pH, and conductivity. Permeate samples were taken at the end of each wastewater effluent feed tests, and periodically when permeate flux behavior was non-uniform, to measure pH, and conductivity.

The PP.2μ membrane was able to successfully produce a clean water flux before and after 2 membrane chemical cleanings. After the third chemical cleaning, the permeate flux trend was inconsistent and sample conductivity values showed that contaminants were breaking through. The SEM and XRD analysis images of the membrane surface and cross-section help to identify the fouling effects on the membrane pores and to help determine how and which contaminants were allowed through. Details of the analysis for each phase can be found later on in section 3.4 and experimental results are found in Chapter 4. A description of the DCMD system design, experiments and the data analysis methods are given in the following sections.

3.2 Data Collection Methods

Data was collected to measure system performance, system efficiency, clean water permeate flux, and to detect if contaminants were able to pass through the membrane

throughout the research. This section explains each of the four research tasks, mentioned in Chapter 2, in greater detail. After reviewing related literature, materials were gathered to construct the system. The data acquired throughout this research was analyzed by using four main equations and by using SEM imagery and XRD analysis. The equations include flux, contaminant percent rejection and flux recovery. SEM images and XRD analysis of membrane surfaces and cross-sections that were virgin, wastewater fouled, and chemically cleaned are shown as a part of experimental results under Chapter 4. These images and contaminant composition identification allowed for further information analysis, by giving an explanation to the collected data. In the following sections, each of the four research tasks is explained in greater detail to help clarify the experimental methods.

3.3 Research Tasks

Task 1: Construct laboratory-scale DCMD system.

Task 1a: Perform Literature Reviews

An review of journal articles relative to MD, membrane fouling and cleaning, and wastewater reuse provided accurate information and insight to the MD process itself and how to set up and conduct legitimate DCMD system experiments. Reviewing multiple studies that had used similar modules for DCMD and other separation processes gave awareness to specific parameters values which provided a general target range for the constructed DCMD system to attempt to achieve. Comparing system parameters and results to previous studies gave validity to the generated data. After gaining a sense of

which items needed to be included in the DCMD set up, a diagram was drawn and an inventory list was created.

Task 1b: Gather Materials and instruments

A laboratory scale system, consisting of a direct contact membrane distillation module was built using the main components shown in Figure 1. Further explanation of the materials and instruments used is given in Tables 3.4 and 3.5 and in the remainder of section 3.3. The process flow diagram below shows the hot loop, indicated by red arrows, and the cold loop indicated by blue arrows. The membrane cell consists of two half-cells with 7 cm x 17 cm x .08 cm cross-flow channel dimensions. Each channel contains a wide net polypropylene spacer and is encompassed by a viton gasket.

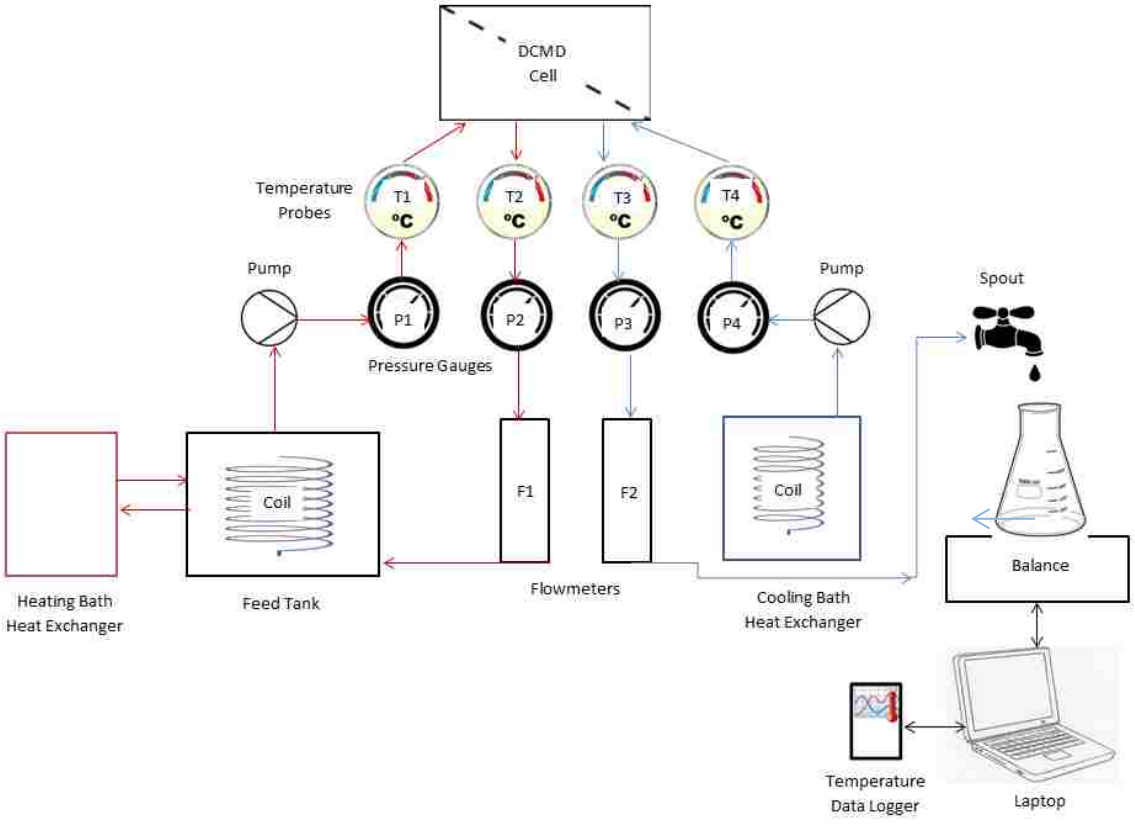

Figure 3.1 Process flow diagram for laboratory scale DCMD system

Table 3.4 DCMD Component and Data Collection Information

DCMD System Data Components	Sub Components	Manufacturer
Membrane Cell	2 Polypropylene half-cells	UNM Mechanical Engineering Shop
	Membranes	See Table 3.2
	2 Gaskets	Gasket Packing and Seal Supply
	2 Channel Spacers	Osmonics
Temperature	Omega 4 Channel Temperature Data Logger	McMaster Carr
	4 Temperature Probes	McMaster Carr
	2 Heating/Cooling Coils	Rupert Pipe Fabricating
	2 Heat Exchangers	Cole Parmer
	1 Feed Tank	US Plastics Corp.
Feed and Permeate Loop Flow Rate	2 Masterflex pumps	Cole Parmer
	2 King Instrument Co. Flow meters	McMaster Carr
Permeate Flowrate	Mettler Toledo Balance	Cole Parmer
	Winwedge Software	TALtech
Pressure	4 Ashcroft Pressure Gauges	Cole Parmer
Conductivity & pH	OaktonPC2700 meter, pH probe, conductivity, and temperature probe	Cole Parmer
TOC Analyzer	Tekmar Dohrmann Phoenix 8000 UV-Persulfate TOC analyzer	Teledyne Tekmar
Membrane fouling	Scanning Electron Microscope and XRD Analyzer	JEOL and Oxford Isis respectively
	K950X Turbo-Pumped Carbon Evaporator for SEM Gold and Palladium Plating	Quorum Technologies

Table 3.5 Membrane Information

Membrane Type	Laminates	Pore Size	Thickness	Manufacturer	Notes
Polytetrafluoroethylene (PTFE)	laminated with PP Scrim	0.22µm	80-170µm	GVS	non-uniform structure, non-porous laminate
Polypropylene (PP)	not laminated	0.22µm	-	GVS	Was not used due to rupturing under pressure of 0-10psi
Polypropylene (PP)	not laminated	0.2µm	103-170µm	Sterlitech	Selected for Membrane Cleaning Tests
Polypropylene (PP)	not laminated	0.1µm	75-110µm	Sterlitech	Non-uniform structure

Further Explanation for Item Selections:

Membrane Configuration and Material

The flat sheet microporous membrane form was chosen for its ease of accessibility for installation, replacement and observation under an SEM as opposed to hollow tube membranes. Polypropylene (PP) and PP scrim laminated polytetrafluoroethylene (PTFE) membranes were chosen because the same materials had been widely used in other direct contact MD laboratory scale systems for their hydrophobic properties, high resistance to feed solutions (El-Bourawi et al), and current membrane manufacture availability.

Membrane Pore Size

Pore sizes of 0.22µm, 0.2µm and 0.1µm were chosen to be used because they fall within the typical range of 0.1µm to 0.6µm and prevent pore wetting (Alkhudhiri 2012, Tomaszewska 2000). The laminated PTFE and PP membranes both with a pore size of

0.22μm were ordered from GVS (also known as Maine Manufacturing) and the 0.2μm and 0.1μm PP membranes were ordered from Sterlitech. The 0.22μ PP membranes from GVS were discarded because they ruptured every use under pressures of 0-10 psi.

Channel Net Spacers

Polypropylene large net spacers were selected to place on both sides of the membrane to help support the membrane, decrease concentration polarization and enhance permeate flux (Phatteranawik et al. 2003, Phatteranawik et al. 2001, Martinez-Diez et al. 1998). This material was readily available in the laboratory from previous research studies.

Membrane Module

To determine dimensions of the channels in the membrane module half-cells, a target cross flow velocity of 1 m/s was selected as a target. This particular velocity value was in acceptable range of values from literature reviews. A membrane length and width of 7 cm by 17 cm was chosen by trial and error to conveniently fit in a compact space and gave a value of permeate flow (Q_p) that was similar to literature reviews. Using the target cross flow velocity of 2 m^2/s and the calculated channel cross-sectional area A_x of 0.518 cm^2 was used to calculate the flow through the channel Q_x of 6.2 L/min, using Eq. 3.1.

$$Q_x = v \times A_x \tag{3.1}$$

A previously used system designed for a plate and frame flat sheet high pressure RO model system had similar flat sheet dimensions as the particular size of membrane area for the DCMD design. With a frame readily available, the existing half-cell plate drawing design was modified to fit the 7 cm by 17 cm membrane along with net spacers on both sides and can be seen in Figure 3.2. The depth of the channel in the half cells was designed to 0.8 mm thick to fit the membrane and both spacers without compressing the membrane.

The cell module drawing design was given to the UNM Mechanical Engineering shop where it was machined of polypropylene. The shop also cut 8 new threaded barbs for the vice. Existing nuts and bolts were used to hold the vice together.

Tubes & Tube Insulation

The target tubing inner diameter was established by using a headloss (h_l) equation by estimating a headloss value of 0.885 ft per 10 ft of tubing (Camron Hydraulic Data handbook pg.3-12). The tubing inner diameter (d_i) was calculated using Equation 3.2, which resulted in the option for 0.25-0.5 inches.

$$h_l = \frac{f(\frac{L}{d_i})(\frac{4Q_x}{\pi {d_i}^2})}{2g} \tag{3.2}$$

During the experimental shake down tests, ¼ inch Masterflex L/S24 silicon cured C-Flex tubing was selected for its flexibility and proclaimed pump ware longevity. However, the

pump heads caused noticeable disintegration marks in the tubing. A white silicon and carbon substance was accumulating heavily in the cell permeate flow pathways and onto the membrane, possibly disrupting the system flow and pressure.

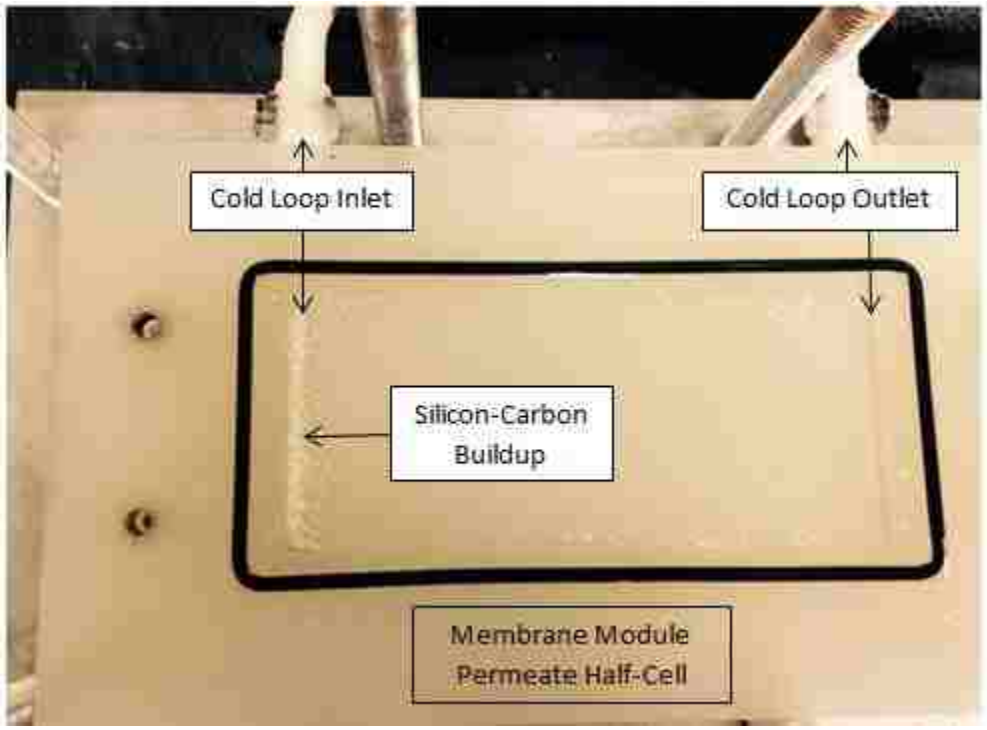

Figure 3.2 Silicon-carbon substance build up in permeate inlet.

The substance was suspected to have been either leaching from the tubing or more likely disintegrating on the inside from the pump friction. This occurred despite the tubing being rotated and replaced between uses. All silicon cured tubing was replaced with transparent Masterflex L/S24 Tygon tubing for the remainder of tests which made the problem go away. Transparent ½ inch hard tubing was selected for smaller length connections for its stability and allowed fluid flow observation. ½ inch thick polyethylene

foam rubber insulation from McMaster-Carr was applied to all tubing to help preserve temperature efficiency.

Tanks & Tank Insulation

Two, 6 gallon, rectangular 14”x10”x10”, 3/16 inch thick PP tanks from Saint-Gobain Performance, were ordered from USPlastic Corp. to hold 10 L of feed solution. Holes of 1-1/8” diameter were drilled for the feed and return lines. The tank outer wall surface area (A_t) was 0.505m^2. The calculated heat transfer coefficient for the material separating two flows (U) was 0.409 W/m°K (Bishop, 2000). A mean temperature difference of the tank water and laboratory atmosphere of 27.2°C was measured and heat transferred per unit time (Q) was found using the heat transfer equation:

$$Q = UA_t\Delta T_m \tag{3.3}$$

The feed tank was calculated to have approximately 884 Watts of heat loss between tank water and laboratory atmosphere. To account for this heat loss, 1 inch thick polyethylene foam rubber insulation from McMaster-Carr was applied to all sides of the tank to help preserve temperature and energy efficiency.

Fittings

A detailed drawing was made to identify and quantify each type of fitting needed and was ordered from USPlastic Corp.

Pressure Gauges

Four Ashcroft, $2^1/_2$ inch dial, 316 stainless steel, back connection, liquid filled, high accuracy pressure gauges were ordered from Cole Parmer.

Heating Baths

An existing Themo Electron Corp. Neslab RTE 7 cooling bath was used to regulate the temperature for the cold permeate loop. A Standard 6.5L, 100C, 115Vac/60Hz heating bath was ordered from Cole Parmer to regulate the temperature for the hot feed loop.

Flowmeters

Two, panel-mount, 316 stainless steel valve, 0.1-1 GPM flowmeters with ¼" NPT female x ½" male fittings were ordered from McMaster-Carr.

Pumps

Two existing Masterflex model number 7524-00 pumps were used to circulate the feed and permeate loops.

Electronic Balance and Balance Recording Software

A New Classic MS Mettler-Toldeo balance ordered from Cole Parmer was connected to a laptop and used Winwedge software to record permeate accumulation.

Thermocouples & Data Logger

A four channel temperature data logger and HH300/115Vac-adaptor were ordered from Omega. Four ¼" NPT (M), 0.5"L, Digi-Sense, type K pipe plug thermocouples were ordered from Cole Parmer.

Coils

Two 3/8" OD, 0.035" thick, 316 stainless steel coils were custom made by Rupert Pipe Fabricating. One was made to fit inside the feed tank and the other to fit inside the cooling bath to serve as heat exchangers.

Task 1c: System Assembly

The final DCMD system assembly is shown in Figure 3.3. A wooden stand was designed and made to hold the two flowmeters, four pressure gauges, temperature gauges, permeate outlet, and the piping and fittings that were connected to the membrane cell. Flexible and hard tubing was laid out and cut to desired lengths and connected by the appropriate Teflon tape wrapped fittings. The feed tank and all hot and cold tubing were covered with insulation.

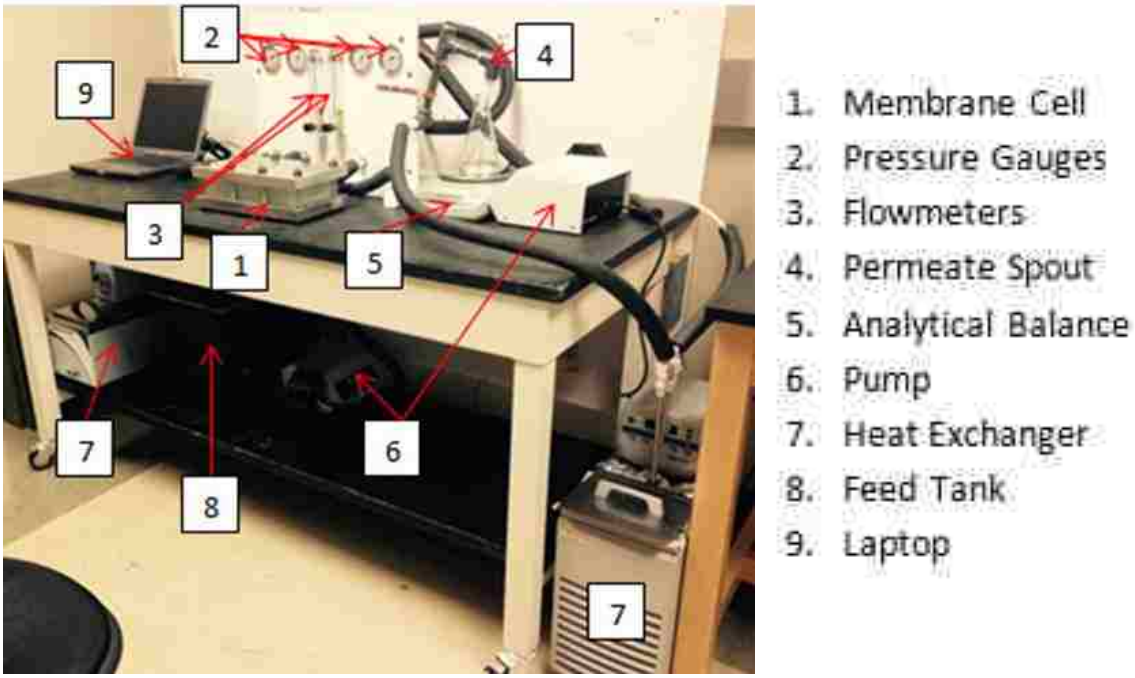

Figure 3.3 DCMD system setup.

Task 1d: Instrument Calibration

Temperature Probe Calibration

All four temperature probes were connected to the cooling bath coil and a pump. The pump was set to 760 mL/min, circulating DI water within the closed loop. The temperature data logger was set to record and the heat exchanger bath was set to 20°C, 30°C, 40°C, and 50°C respectively. The temperature recorded for about ten minutes before changing to the next temperature. Figure 3.4 shows the initial temperature test.

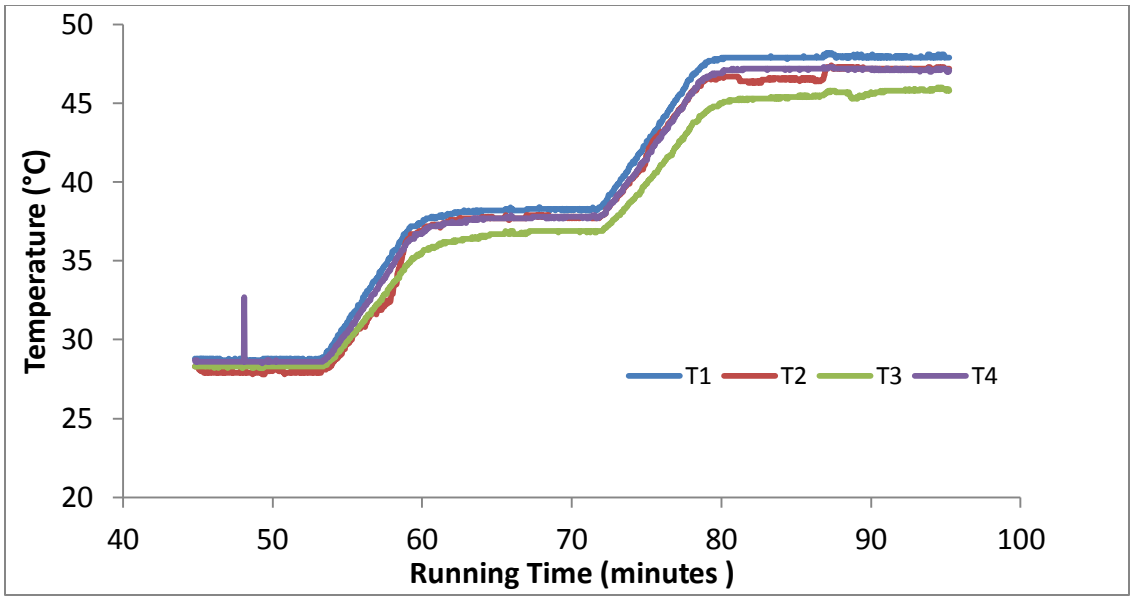

Figure 3.4 Temperature calibration test results for initial four temperature probes.

Testing results confirmed that temperature probes T2 and T3 needed to be calibrated. T3 differed from the other three probes, especially at temperatures higher than 38°C. They were manually calibrated using an ice water bath. T2 did not need an adjustment, but T3 was adjusted by 2°C. The calibrated temperature test results are shown in Figure 3.5. After calibration T3 still lacked accuracy to measure temperatures above 40°C. It was replaced by a new accurate probe.

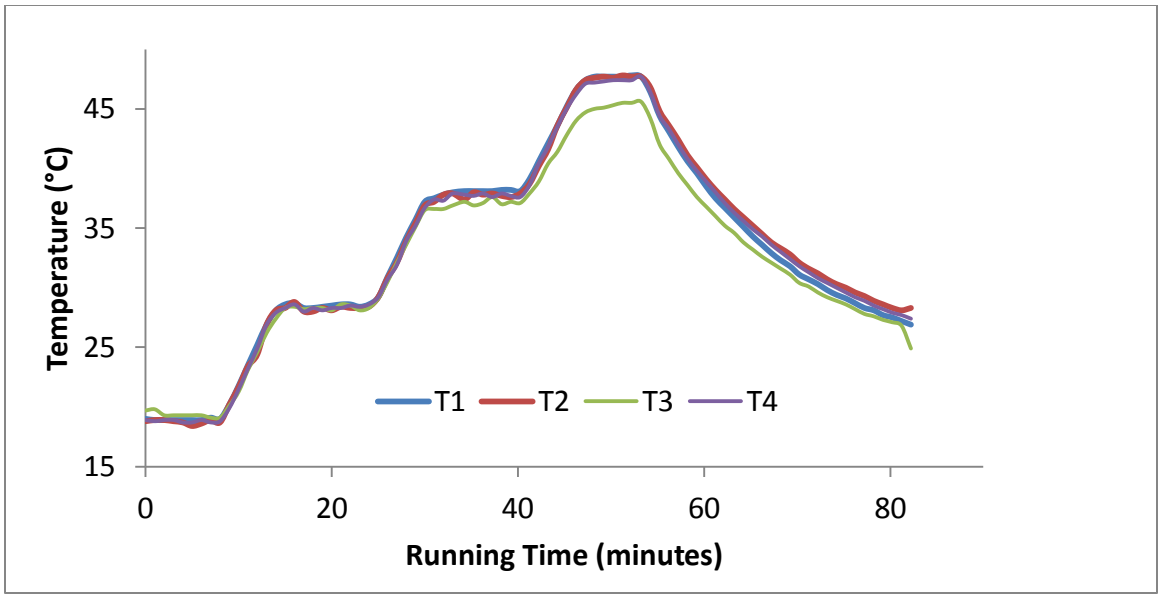

Figure 3.5 Temperature test results after temperature probe calibration.

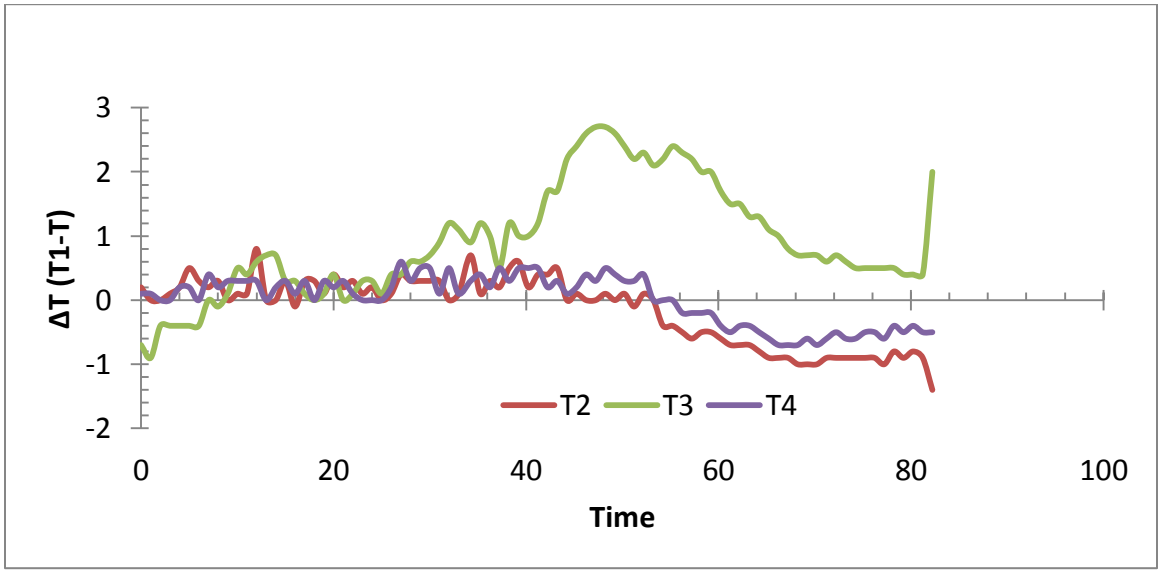

Figure 3.6 Temperature difference between a chosen baseline probe (T1) and T2, T3, and T4. These results were produced after calibration, indicating T3 needed to be replaced.

Flowmeters and Pump Calibrations

The two flowmeters were each calibrated separately using the following procedure. The meter was connected to a pump. The pump flowrate was adjusted until the pump the flowmeter read 0.2, 0.3 and 0.4 GPM respectively. The flowrate was measured experimentally by collecting a volume of water over a defined time, and compared to the flowrates of the flowmeter and pump. The flowrate for the meter, pump, and calculated flowrate were recorded and are shown in Table 3.6. The calibration data for flowmeters 1 and 2 are found in table 3.6 and 3.7 respectively. Despite the fact that pulse dampeners were unavailable, resulting in a vibrating meter float, there was good correlation between the measured flows and the flow display values on the pump and flowmeter. The pump calibration curves are shown in Figures 3.8 and 3.10, and the flowmeter calibration curves are shown in Figures 3.7 and 3.9.

Table 3.6 Calibration Data for Flowmeter 1

Flask (g)	Flowmeter (GPM)	Pump (mL/min)	Time (sec)	Flask + Water (g)	Water (g)	Water (mg)	Water (mL)	Time (min)	Measured Flow (mL/min)	Measured Flow (GPM)
460	0.215	720	100.35	1698.7	1238.7	1238700	1241.18	1.67	742.11	0.20
463.5	0.21	710	93.2	1588.2	1124.7	1124700	1126.95	1.55	725.51	0.19
462	0.2	680	108.44	1722.1	1260.1	1260100	1262.63	1.81	698.61	0.18
462.1	0.3	1100	67.66	1700.2	1238.1	1238100	1240.58	1.13	1100.13	0.29
462.5	0.4	1540	49.53	1785.8	1323.3	1323300	1325.95	0.83	1606.24	0.42

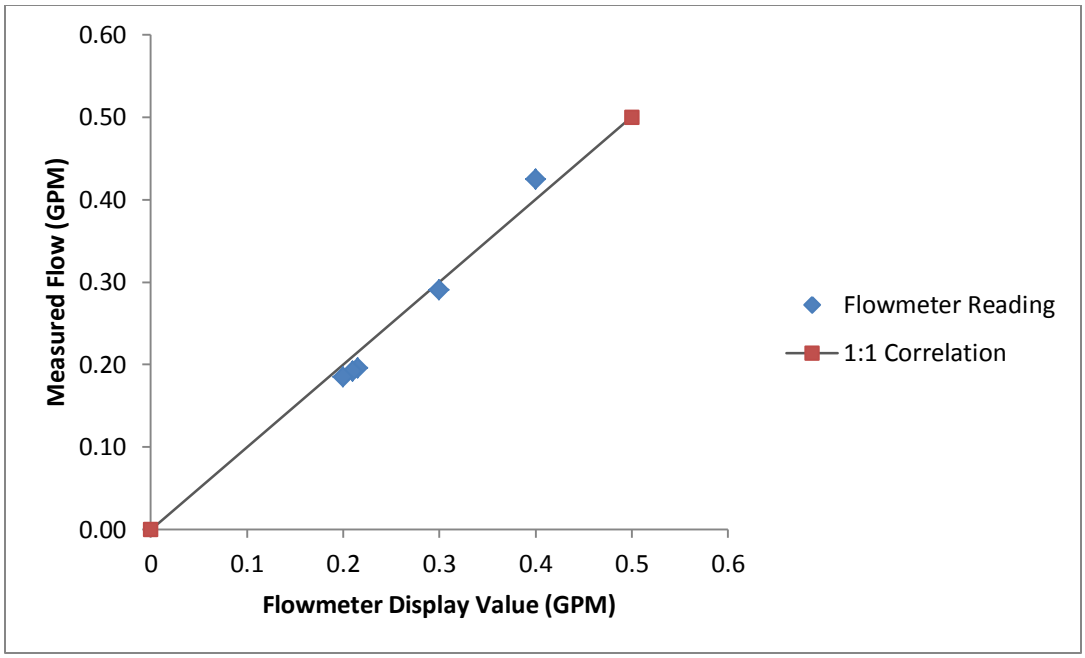

Figure 3.7 Flowmeter 1 calibration curve.

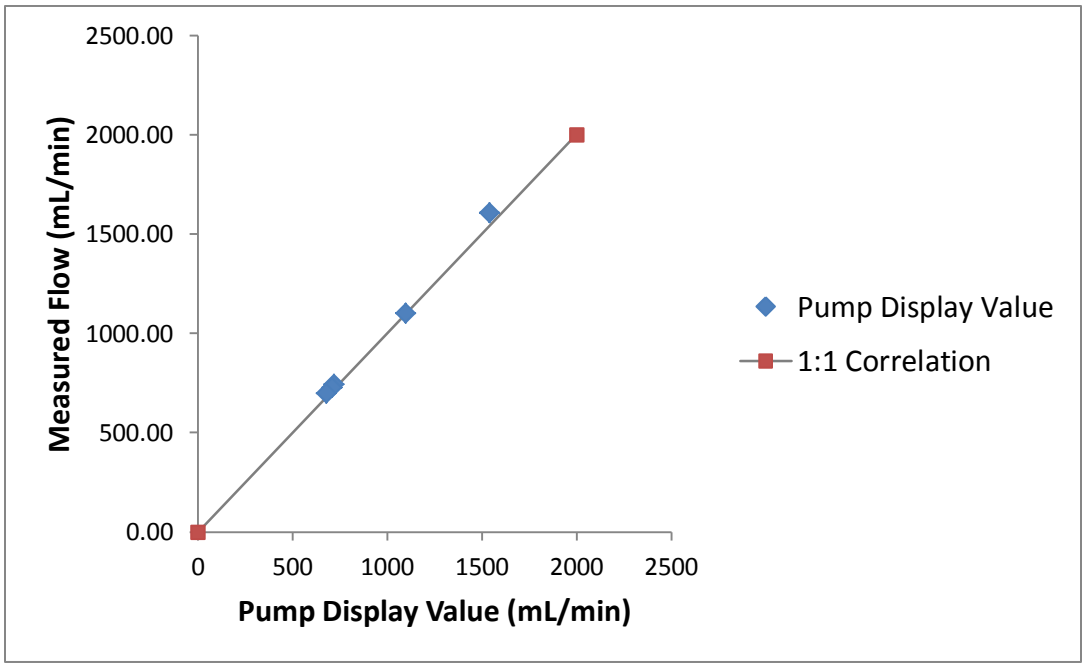

Figure 3.8 Pump 1 calibration curve.

Table 3.7 Calibration Data for Flowmeter 2

Flask (g)	Flowmeter (GPM)	Pump (mL/min)	Time (sec)	Flask + Water (g)	Water (g)	Water (mg)	Water (mL)	Time (min)	Measured Flow (mL/min)	Measured Flow (GPM)
460.7	0.22	680	64.26	1187.2	726.5	726500	727.96	1.07	679.70	0.18
463	0.24	740	80.31	1437.6	974.6	974600	976.55	1.34	729.59	0.19
462.5	0.28	1050	60.08	1490.3	1027.8	1027800	1029.86	1.00	1028.49	0.27
462.6	0.3	1120	55.86	1485.2	1022.6	1022600	1024.65	0.93	1100.59	0.29
462.3	0.32	1240	49.68	1470.5	1008.2	1008200	1010.22	0.83	1220.07	0.32
462.1	0.4	1540	37.91	1454	991.9	991900	993.89	0.63	1573.02	0.42

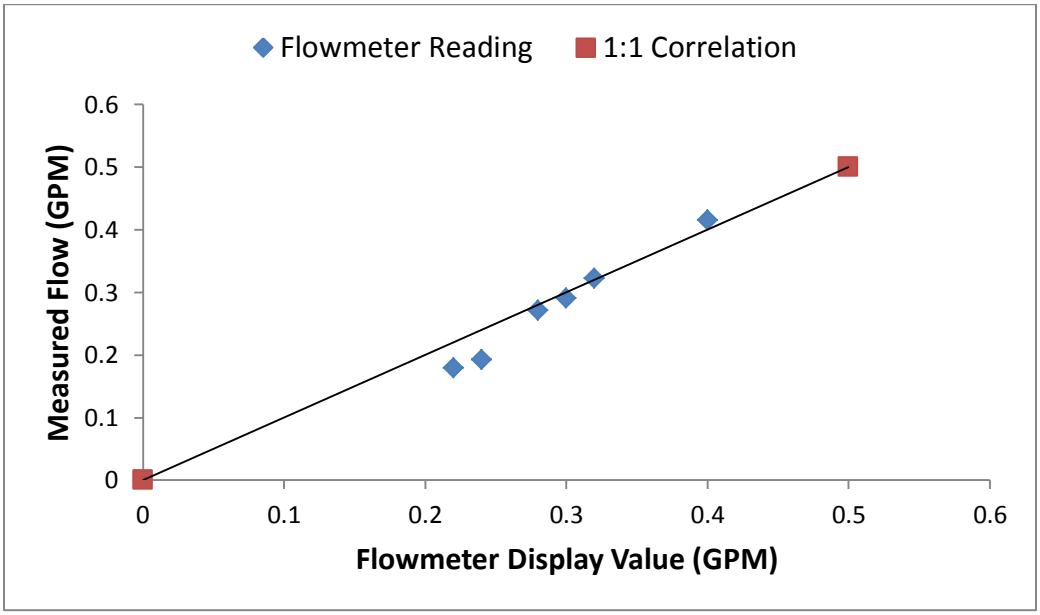

Figure 3.9 Flowmeter 2 calibration curve.

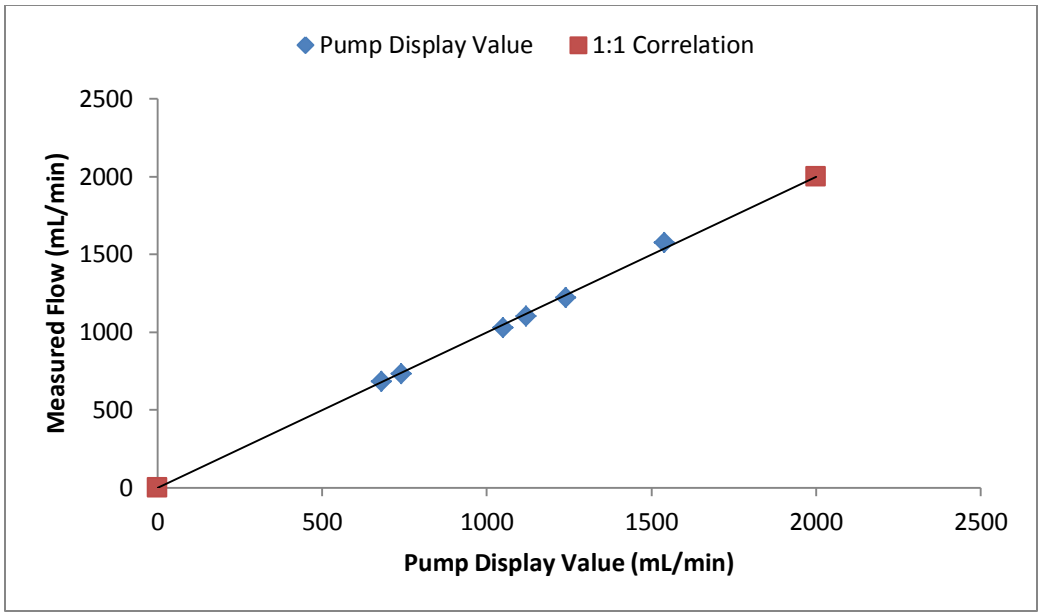

Figure 3.10 Pump 2 calibration curve.

Pressure Gauge Calibration

All four pressure gauges were connected together by fittings, and flexible tubing to a coil within a cooling bath, and pump. The pump was set to 760 mL/min, circulating 20°C DI water. The temperature data logger was set to record and the pump was set to 760, 900, 1000, 1120, 1300, 1400, and1500 mL/min and the values were recorded for all gauges at each speed as seen below in Table 3.8 and 3.9. Figure 3.11 shows the data with a faulty gauge, and 3.12 shows the data with a replacement gauge. Figure 3.13 shows gauge 1 as a baseline with respect to the other three gauges.

Table 3.8 Initial Pressure gauge calibration data.

Gauge 1	Gauge 2	Gauge 3	Gauge 4	Pump Reading (mL/min)	Flowmeter Reading (GPM)	mL/min converted to GPM Check
0	0	0.05	0	0	0	0
1.2	0	2.1	1.6	760	0.185	0.200770759
1.6	0	2.6	2.4	900	0.22	0.237754846
2.1	0	3.2	3.1	1000	0.255	0.264172051
2.9	0	4	4	1120	0.29	0.295872697
3.8	1.1	4.9	5.09	1300	0.34	0.343423667

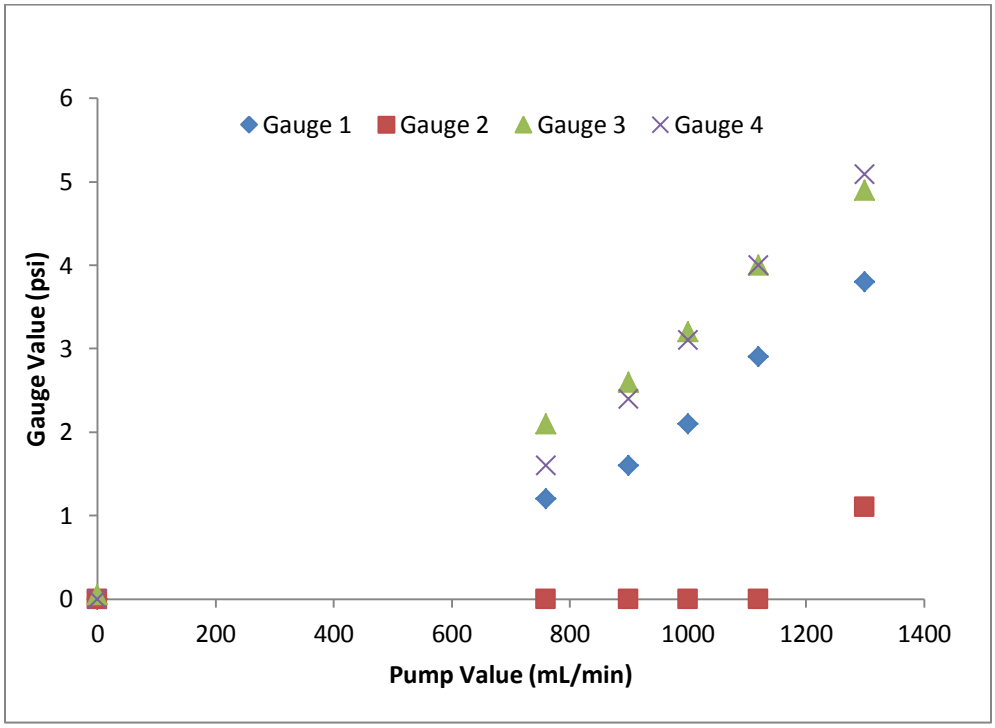

Figure 3.11 Initial pressure gauge calibration results.

After replacing the dysfunctional pressure gauge 2, all four were tested again. As seen in Figures 3.12 and 3.13, the pressure gauges were all in an acceptable range within each other, insuring that they were reading pressures accurately.

Table 3.9 Pressure gauge calibration data with the replaced gauge.

Pump speed (mL/min)	Gauge 1	Gauge 2	Gauge 3	Gauge 4
0	0	0	0	0
760	0.6	0.1	0.4	0
900	1.25	0.2	0.9	0.1
1000	1.4	0.5	1	0.3
1120	1.8	1	1.4	0.9
1300	2.4	1.6	2	1.7
1400	2.5	1.75	2.2	2
1500	2.65	1.9	2.4	2.15

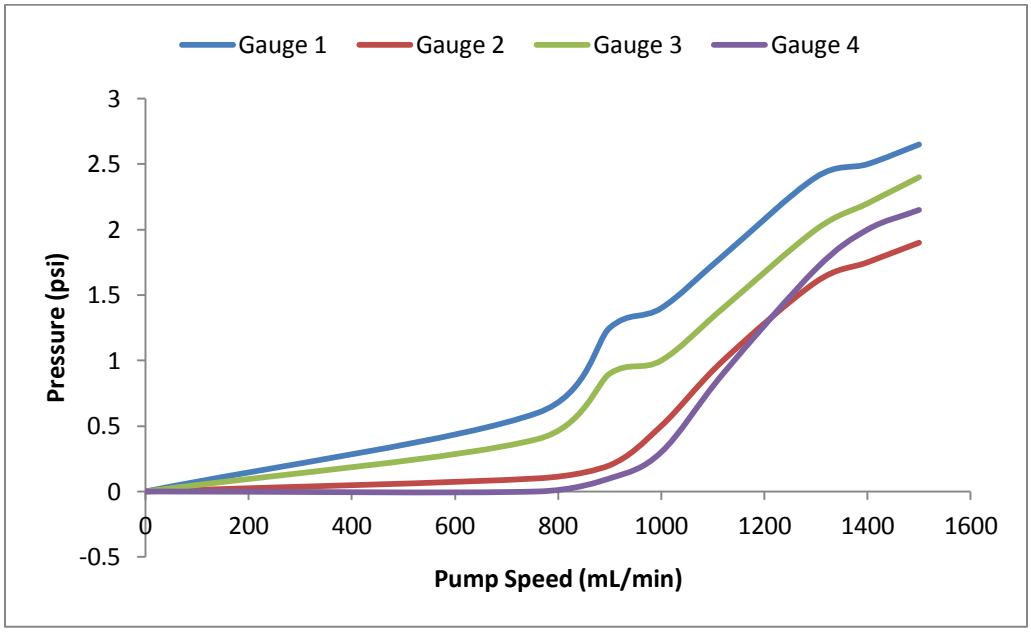

Figure 3.12 Second pressure gauge calibration test results.

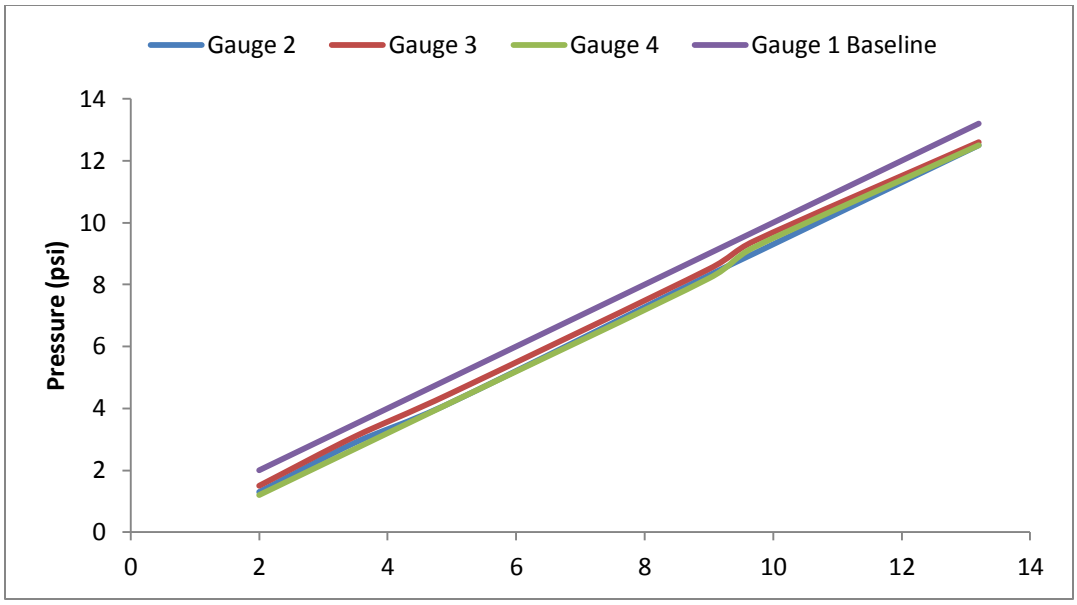

Figure 3.13 Pressure values of gauges 2, 3 and 4 with respect to 1 as the baseline. These results are from the second calibration test.

Task 2: Evaluate the performance of the MD system relative to performances that has been reported in peer-reviewed literature.

Initial Testing

Once all of the instruments and devices included in the DCMD system were tested and calibrated to assure data collection accuracy, initial testing was conducted to gather information about the effects of the systems parameters. Multiple tests were performed with a feed solution of DI water, salt solution, and wastewater effluent and are shown in Tables 3.1 and 3.2. The permeate loop was flushed with fresh DI water at the beginning of each test. Once the system produced a steady permeate flux, the temperature and flux was set to record every minute. Each test in phase one was run and monitored for approximately an hour. The temperature settings on the heat exchanger baths were adjusted periodically as needed to maintain the desired feed temperature and delta T.

DI Water Feed & DI Water Permeate

The first shakedown test was performed with DI water in both hot and cold loops to check system functionality. Leaks were eliminated by inspecting the system during operation for water drips and bubbles. A steady permeate flux was observed in as little as 2 minutes of operation. Delta T was established by observing T1 (feed inlet temperature) and T3 (permeate inlet temperature) values and adjusting the heating and cooling baths accordingly.

500 mg/L NaCl Feed and DI Permeate

10L of 500mg/L NaCl feed solution was prepared by mixing 5g of NaCl into 10L of DI water. Temperature and permeate flux data were recorded at 1 minute intervals for an hour. Experiments that were run with the NaCl feed solution are shown in Table 3.1. The data was graphed in excel to calculate running time, delta T, permeate flux, and system efficiency. The equations used to calculate these values are discussed in section 3.4 Experimental Analysis Methods. Results of the testing parameters are discussed in Chapter 4.

The overall function of the system was analyzed by methodically comparing system performance to that previous research with DCMD laboratory scale systems. The main system properties that were compared were crossflow velocity, feed temperature, delta T, exposed membrane area, feed solution type and concentration, system rejection, permeate flux values and behavior, and membrane fouling and scaling effects on permeate flux. By systematically comparing properties and functionality of both the constructed DCMD

with preexisting MD systems, verification that the system functioned correctly, was assured.

Task 3: Investigate fouling of wastewater effluent on DCMD membranes.

A wastewater effluent feed solution was obtained from the ABCWUA South Side Wastewater Reclamation Plant outfall. The effluent solution characteristics are shown in Table 3.10.

Table 3.10 NPDES Report for wastewater effluent collected on from ABCWUA SWRP on 3/12/2015 and monthly averages

Parameter	Value	Monthly Average for Void Daily Value
Effluent Flow (MGD)	51	
Highest Hourly Flow (MGD)	63.5	
Influent Alkalinity (MG/L)	270.4	
Influent Ammonia (MG/L)	-	40.65
Effluent Nitrogen, Ammonia total (as N)	0.1	
Influent TSS (MG/L)	372	
Effluent TSS (MG/L)	7	
Influent cBOD (MG/L)	-	320.6
Effluent cBOD (MG/L)	-	3
Aer MLSS Lab (mg/L)	4700	
Effluent Nitrate Nitrite (MG/L)	9.5	
Effluent TIN (mg/l)	9.6	
UTV (mJ/cm2)	71.3	
Effluent (µg/L)	-	0.0016
E-Coli (mpn/100)	1	
Effluent D.O. (mg/l)	6.2	
Effluent TRC (MG/L)	<0.03	
Effluent pH	6.9	
Flow weighted ALK (mg/l)	95.3	

The wastewater effluent test details for this section are shown in Table 3.2. 10 L of the wastewater effluent was put into the feed tank. The collected data was graphed in excel to calculate running time, delta T, permeate flux, and system efficiency. Results of the testing parameters are discussed in Chapter 4. Temperature and permeate flux data were recorded at 1 minute intervals. Only the 0.22μm PTFE and 0.1μm PP membranes were used due to availability. The data was graphed in excel to calculate running time, delta T, permeate flux, and system efficiency. The equations used to calculate these values are discussed in section 3.4. Results of the testing parameters are discussed in Chapter 4.

Task 4: Investigate the effect of chemical cleaning on membranes fouled by wastewater effluent.

Membrane Fouling and Cleaning

Testing procedures were the same as above, and involved filling the feed tank with 10L of wastewater effluent. The test details for this section are shown in Table 3.3. Temperature and permeate flux data were recorded at 1 minute intervals throughout the wastewater fed tests. Only the 0.1μ PP membrane was used to limit test variability. The reasons why this membrane was selected is discussed in Chapter 5. The data collected from these tests was graphed to calculate running time, delta T, permeate flux, and system efficiency. The equations used to calculate these values are discussed in section 3.4. Results of the testing parameters are discussed in Chapter 4. The steps in the cleaning process are listed below:

Membrane Chemical Cleaning Process:

1. Determine Initial Membrane Flux

- Set up system with Tank 1:
    - Feed solution: 10L Wastewater effluent
    - Permeate Solution: DI water
    - Feed Temperature: 70°C (to help induce fouling)
    - Delta T: 20°C
    - Feed and Permeate crossflow velocity: 0.15 m/s (to help induce fouling)
    - Place extra tank on balance to collect permeate
- Take a sample of DI loop water and wastewater effluent feed to analyze pH and conductivity
- Once the temperatures T1 and T3 meet their target and there is a steady flux, start recording temperatures on data logger and balance readings in Winwedge
- Average the first 90 minutes of balance readings to get an initial permeate flow rate in g/minute. Calculate flux in L/m2h.

2. Membrane Fouling

- Allow system to run continuously until the permeate flow rate is approximately 50% of the initial permeate flow rate.
- After the permeate flow rate reaches 50%, take a permeate sample and wastewater effluent sample for pH, and conductivity analysis
- Stop all recordings and stop the system
- Disconnect wastewater effluent feed Tank 1 and close off openings with clamped soft tubing

- Rinse coil with DI

3. Chemical Cleaning

- Fill Tank 2 with 2-3L of DI water and connect the outgoing feed tube (tube with the pump) and place the return tube end in an empty bucket
- Flush trapped wastewater with DI and displace in a bucket and dispose
- Empty remaining DI water from Tank 2
- Prepare the following cleaning solution and add 1M NaOH to achieve a pH of 11
- Fill permeate tank with following feed solution and set up system:
    - Feed solution: 5L of 2mM EDTA, pH 11 (adjusted pH with NaOH)
    - Permeate Solution: DI water
    - Feed Temperature: 70°C
    - Delta T: (70°C-cleaning solution temperature at room temp)
        - Keep unused cooling bath set to 20°C settings
    - Feed Crossflow velocity: 0.15 m/s, Permeate crossflow velocity: 0.0 m/s
- Run the pumps for 15 minutes once solution reaches 70°C
- Stop the system
- Rinse the coil with DI
- Empty and wash Tank 2 and fill with 2-3L DI water
- Connect the outgoing tubing to the permeate tank and place the incoming tube into the bucket
- Flush cleaning solution out of feed side and dispose
- Flush the permeate side with 2-3L DI water into the bucket and dispose

4. Post Cleaning Membrane Flux

- Connect the wastewater effluent feed Tank 1
- Fill Tank 1 with fresh wastewater effluent
- Assure permeate loop is full with DI water
- Set up the system:
    - Feed solution: 10 L Wastewater effluent
    - Permeate Solution: DI water
    - Feed Temperature: 70°C
    - Delta T: 20°C
    - Crossflow velocities: 0.15 m/s
- Once T1 and T3 reach their goal temperatures and a steady flux is present, start recording the permeate flow rate and temperature.
- Collect wastewater and permeate samples to analyze pH, and conductivity
- Average the first 90 minutes of balance readings to get an initial accumulation in g/minute. Calculate flux in L/m2h.
- Once the permeate flow rate reaches the original 50% flux decline value, collect a permeate and wastewater feed sample to analyze pH and conductivity
- Stop system and recordings
- Repeat the rest of steps 2-4 until membrane is cleaned and re-fouled up to a point of system failure.

5. Analyze results

Note that the first membrane cleaning test series shown in Table 3.3 only went through one cycle of the cleaning procedure due to an increase in permeate conductivity that is

shown in Chapter 4. The second cleaning tests included three membrane cleaning cycles before a permeate conductivity increase occurred. The second cleaning test series also included a decrease of chemical solution feed temperature and crossflow velocity as well as a cleaning time increase as was discussed in section 3.1.

3.4 Data Analysis

For all of the tests shown in the three experiment matrixes, calculations were done to determine the permeate flux, contaminant rejection, system energy efficiency, and flux recovery after membrane cleanings. Scanning Electron Microscopy (SEM) and an XRD analysis was also used to help identify membrane foulants. The pH and conductivity were measured with an Oakton PC2700 meter mentioned in Table 3.4. The conductivity was measured three times and averaged for consistency. The TOC was measured using the Tekmar Dohrmann Phoenix 8000 UV-Persulfate TOC analyzer also mentioned in Table 3.4. Because details of the TOC analysis procedure were unable to be resolved, the data has been excluded. The equations and measurement preparation procedures are given in detail below.

Equations Used

Permeate Flux

$$J_p = {Q_p}/{A_m} = C(\Delta V) \tag{3.4}$$

Where

$J_p = Permeate\ Flux\ ({L}/{m^2 h})$

$Q_p = Permeate\ Flowrate\ (^{L}/_{h})$

$A_m = Effective\ Membrane\ Area\ (m^2)$

$C = Membrane\ Distillation\ Mass\ Transfer\ Coefficient\ \left(^{L}/_{kPa \cdot m^2 h}\right)$

$\Delta V = Vapor\ Pressure\ Differential\ (kPa)$

Contaminant Rejection (%)

$$(1 - \frac{\sigma_{permeate}}{\sigma_{feed}}) * 100 = \%\ of\ Contaminant\ Rejection \quad (3.5)$$

where

$\sigma = Sample\ Conductivity\ (^{\mu S}/_{cm})$

System Energy Efficiency (%)

$$\%\ Energy\ Efficiency = \frac{E_V}{E_C} * 100 \quad (3.6)$$

where

$$E_V = Energy\ of\ Vaporization = \Delta H_V / MW_w * \rho_w * Q_p \quad (3.7)$$

$$E_C = Total\ Energy\ Released = C_P / MW_w * \rho_w * Q_x * \Delta T \quad (3.8)$$

where

$MW_w = Molecular\ Weight\ of\ water\ (^{g}/_{mol})$

$\rho_w = Density\ of\ water\ (^{g}/_{L})$

$Q_x = Channel\ crossflow\ velocity\ (^{L}/_{min})$

$C_P = Heat\ Capacity\ of\ water\ (^{kJ}/_{g°C})$

$\Delta H_V = Enthalpy\ of\ Vaporization\ of\ Water\ (^{kJ}/_{mol})$

$$\Delta T = Feed\ inlet\ temperature - Permeate\ outlet\ temperature\ (°C) \quad (3.9)$$

Flux Recovery (%)

$$\% \, Flux \; recovery = (1 - {}^{J_i}/_{J_o}) * 100 \tag{3.10}$$

where

$J_o = Initial \; Flux \; ({}^{L}/_{m^2 h})$

$J_i = Initail \; Flux \; after \; (i) \; membrane \; cleanings \; ({}^{L}/_{m^2 h})$

SEM and XRD Analysis

Samples of fresh and fouled membranes were examined by SEM and XRD to determine the nature of the material accumulating on the fouled membranes. To prepare the membrane surface samples, pieces of each membrane were cut and fixed onto carbon paper. For the membrane cross-sections, a strip of the membranes were soaked in liquid nitrogen and then cracked on a hard surface before they were placed on the carbon paper. All samples were plated with a gold and palladium coating with a K950X Turbo-Pumped Carbon Evaporator for SEM. The SEM images produced a microscopic image of patterns and textures on the membrane surfaces and the XRD analysis provided elemental composition identification. SEM imagery and XRD analyses graphs, allowed for membrane fouling constituent classification. The SEM images, XRD constituent component results, and experimental results are shown and discussed in Chapter 4.

Chapter 4 Experimental Results

4.1 System Parameter Definitions

Four temperatures located near the membrane cell feed inlet (T1) and outlet (T2) and near the permeate inlet (T3) and outlet (T4) were recorded for each test. Feed temperature refers to the temperature of the feed solution at the inlet (T1) of the membrane cell. The feed solution temperature decreased as it traveled across the membrane cell between the inlet and outlet is partially due to the enthalpy of evaporation and conductive heat loss. The permeate solution temperature increased across the membrane cell between the inlet and outlet. This temperature change was partially due to condensation of the distillation process and conductive heat transfer. The energy required to vaporize water is shown in Equation 4.1 where E_v (kJ/min) is the energy of vaporization, ΔH_v (kJ/mol) is the enthalpy of vaporization of water, MW_w (g/mol) is the molecular weight of water, ρ_w (g/L) is the density of water and q (L/min) is the permeate flowrate.

$$E_v = \left(\Delta H_v * \rho_w * q \,/\, MW_w\right) \tag{4.1}$$

The heat loss is found by taking the total energy released (E_r) (kJ/min) from the water molecule on the feed side, shown in Equation 4.2, and finding the difference between this total energy and the energy of vaporization. The heat capacity of water is represented by C_p (kJ/mol°C) and q_x (L/min) is the crossflow velocity.

$$E_r = \left(C_p * \rho_w * q_x \,/\, MW_w\right) \tag{4.2}$$

The efficiency is the ratio of the energy that is used for vaporization and the total energy released by the process calculated by Equation 4.3:

$$Efficiency\ \% = {}^{E_v}/_{E_r} * 100 \quad (4.3)$$

The energy lost by the feed solution and gained by the permeate solution that is not accounted for by the enthalpy of evaporation and condensation is due to the convective heat loss through the membrane and represents a reduction in energy efficiency. The transmembrane temperature (ΔT) refers to the difference in temperature between the feed inlet solution and the permeate outlet solution. This represents the difference in temperature of the solutions separated by the membrane.

Permeate flux (J) (L/m^{2}h), and the water mass transfer coefficient (*C) (*L/m^{2}h·kPa), which involves temperature, membrane characteristics, and solute characteristics. The transmembrane vapor pressure differential is represented by ΔV_p (kPa), which is dependent on ΔT.

$$J = C(\Delta V_p) \quad (4.4)$$

These equations and relationships were used to interpret the experimental results.

4.2 Experiment Overview

Each test shown in the experiment matrices in Tables 3.1, 3.2, and 3.3 was graphed using the recorded feed temperature, ΔT, and permeate flux data. The feed temperature and ΔT were graphed using the raw data, and the permeate flux was graphed using a running average. Figure 4.1 shows an example of the first NaCl test. The remaining graphs in this chapter show averaged feed temperatures and permeate flux resutls.

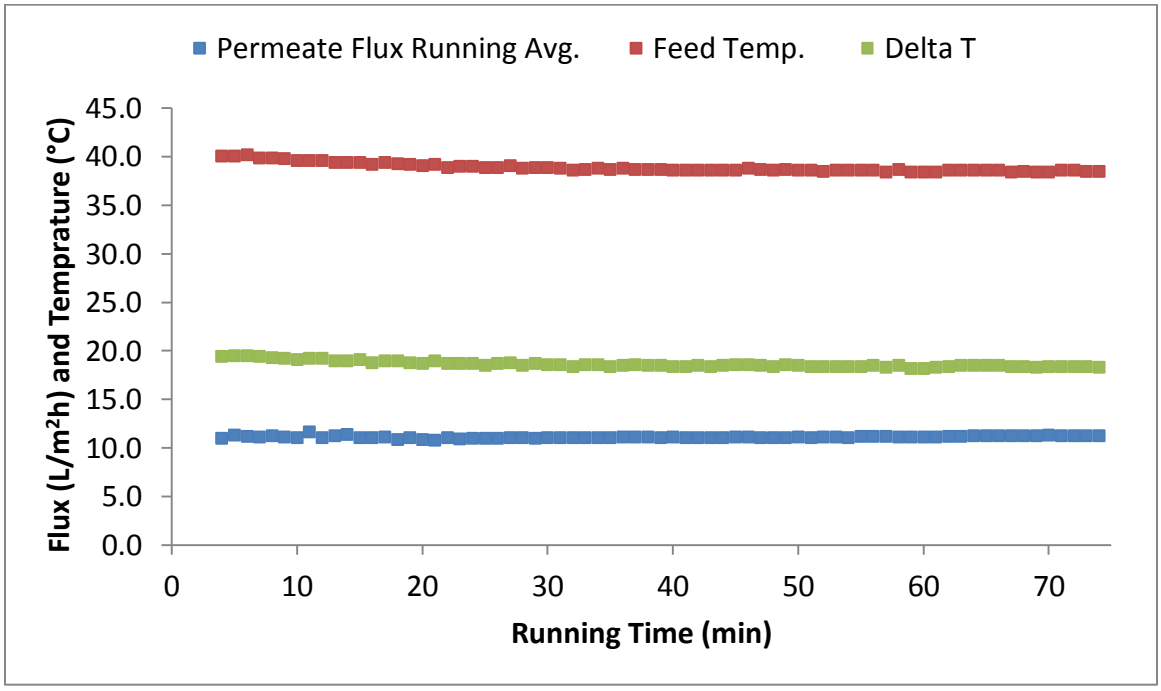

Figure 4.1 NaCl test 1. 500 mg/L NaCl feed solution, 0.22µm PTFE membrane, feed temperature of 40°C, ΔT of 20°C, and channel crossflow velocity of 0.24 m/s.

The experiments were done in three phases. Phase one included the investigation of the DCMD system's properties and functionality with regards to various parameters. Hydraulic tests were performed to check to leaks and function. To determine the effects of channel crossflow velocity, transmembrane temperature (ΔT), feed temperature and membrane type on the permeate flux, 16 tests were run using a 500 mg/L of NaCl feed

solution. Phase two used effluent from the Albuquerque Bernalillo County Water Utility Authority (ABCWUA) Southside Wastewater Reclamation Plant (SWRP) as the feed solution for 8 tests, for which 3 could be compared to NaCl feed tests to compare the effects of feed solution type.

Phase two evaluated membrane fouling when treating municipal wastewater effluent but also related system parameters to permeate flux. Only 1 out of the 8 wastewater effluent tests resulted in flux decline due to membrane fouling and is discussed below. Phase three investigated the effects of a chemical cleaning on wastewater fouled membrane. The first cleaning test involved running treated wastewater as the feed solution for 8.5 hours until the flux declined by 54%. The cleaning process was run and followed by running a treated wastewater feed solution again. A flux recovery of 92%was observed. Despite this high recovery percentage, the chemical cleaning testing had to have a few of the parameters adjusted for the second test, further explained in section 3.4. The second test had two successful membrane cleanings that recovered 98% and 97% recovery of the initial flux respectively, with >99.9% contaminant rejection for both. The third sequential cleaning resulted in low levels of dissolved ions passing through the membrane, giving 99.9% rejection at the beginning of the test that eventually decreased to 96% contaminant rejection towards the end of the test. Tabulations and figures of data, SEM images, and EDS graphs are shown below and explained further for each of the three phase results in section 4.4.

4.3 Phase one: System Parameters

Phase one included tests 1-16 of the 500mg/L of NaCl feed solution from the experiment matrix. Membrane specifications, crossflow velocity results, ΔT results, and feed temperature for each of the three membranes are shown in section 4.1a. Three NaCl tests are compared to three treated wastewater tests to compare feed solution types. Table 4.4 shows the system efficiencies from phase one and also includes phase two efficiencies for comparison.

4.3a Membranes

A PTFE and two PP membranes were used in phase one for this study, with specifications shown in Table 4.1. These specific microfiltration membranes were used for their hydrophobicity, liquid surface pressure resistance, hydraulic pressure resistance, and pore diameters to help prevent pore liquid penetration (Gryta 2005, Cath et al. 2004). SEM images of new membrane surfaces are shown to get a better understanding of their structure and texture.

Table 4.1 Membrane Specifications

Membrane Type	Manufacturer	Laminates	Pore Size	Thickness
Polytetrafluoroethylene (PTFE)	GVS	laminated with PP Scrim	0.22µm	80-170µm
Polypropylene (PP)	Sterlitech	not laminated	0.2µm	130-170µm
Polypropylene (PP)	Sterlitech	not laminated	0.1µm	75-110µm

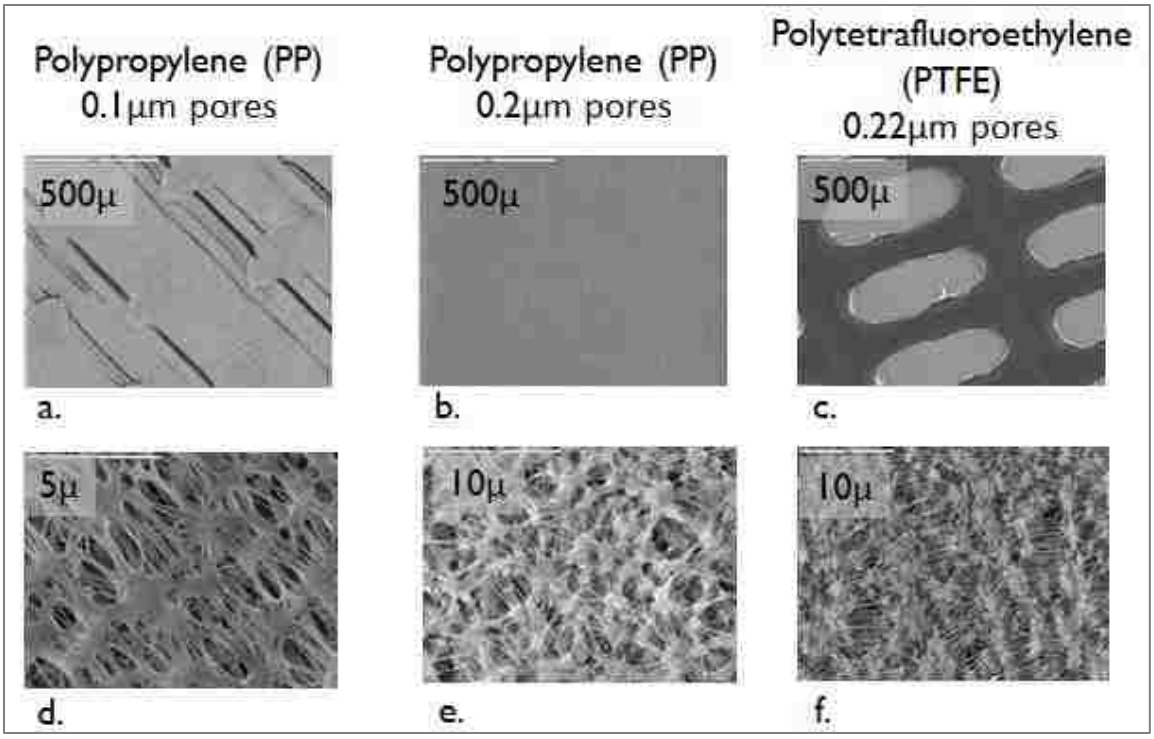

Figure 4.2 SEM images of virgin membrane surfaces. Images include (a) 0.1 µm PP magnified 100x, (b) 0.2 µm PP magnified 100x, (c) PTFE .22 magnified 65x, (d) 0.1 µm PP magnified 10,000x, (e) 0.2 µm PP magnified 5,000x and (f) 0.22 µm PTFE membrane magnified 3,500x.

It appeared as if the 0.1 µm PP membrane had material 'strips' patched together, resulting in a non-uniform surface. The 0.2 µm PP from Sterlitech appears smooth and uniform, though images in the membrane cleaning section show oval patterns on the feed side of the membrane. The image in 4.2b only shows the permeate side of the membrane. The 0.22 µm PTFE from GVS (also known as Maine Manufacturing) was laminated with a non-porous PP scrim laminate, which covered approximately 60% of the surface. Because of availablity, the 0.22 µm PTFE membrane was used consistantly for the parameter testing for crossflow velocity and Δ T testing.

4.3b Crossflow Velocity

Three different channel crossflow velocities of 0.24, 0.29, and 0.39 m/s were investigated using the 0.22µm PTFE membrane and 500 mg/L NaCl feed solution. A plot of the averaged permeate fluxes for each crossflow velocity produced a perfect positive, linear correlation, is shown in Figure 4.3. The effect of increasing the crossflow velocity is to decrease the size of the boundary layers and as a result decreasing the temperature loss in the boundary later, such that the membrane temperature is closer to the solution bulk temperature when the velocity is higher. As a result, the vapor pressure differential higher when the cross-flow velocity is higher. Therefore, the flux is proportional to the crossflow velocity to the first power and as the crossflow velocity increases, the flux increases linearly.

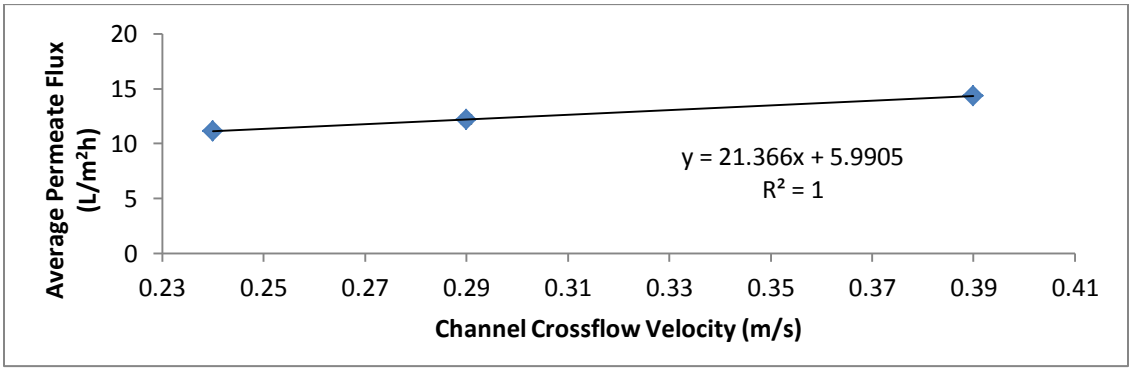

Figure 4.3 NaCl test 1, 7, &8. 500 mg/L NaCl feed solution, 0.22µm PTFE membrane, feed temperature of 40°C, ΔT of 20°C, and channel crossflow velocity of 0.24, 0.29, and 0.38 m/s. The vertical error bars represent one standard deviation of the average permeate flux.

4.3c Δ T

Three Δ T values of 20, 25, and 30°C were investigated using the 0.22 µm PTFE membrane and 500 mg/L NaCl feed solution. Shown in Figure 4.4, the permeate flux

increased linearly as ΔT increased. This positive linear relationship between the two parameters is consistent with El-Bourawi et al and their 51 supporting studies.

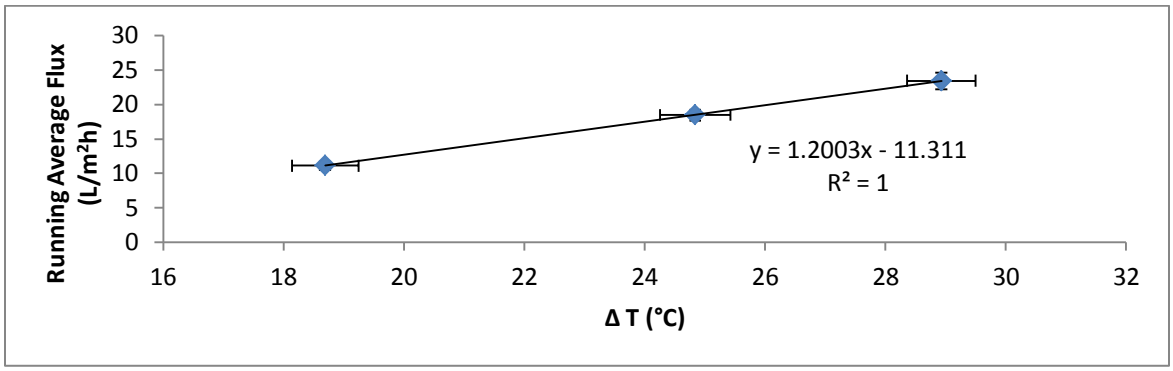

Figure 4.4 NaCl test 1, 5, and 6. 500 mg/L NaCl feed solution, 0.22µm PTFE membrane, feed temperature of 40, 45, and 50°C, ΔT of 20, 25 and 30°C, and channel crossflow velocity of 0.24 m/s. Error bars represent one standard deviation of the ΔT and average permeate flux.

Data points from phase two tests 2 and 3 using the wastewater effluent feed were graphed to investigate the correlation for a constant feed temperature and varying permeate temperature. The permeate solution temperature was held constant at approximately 20°C, while the feed temperature was adjusted to achieve the different ΔT's. Even though the feed solution was different, and involved a wider range of ΔT's, there was still a positive linear relationship between ΔT and permeate flux shown in Figure 4.4. Results for the wastewater effluent feed are shown in Figure 4.5.

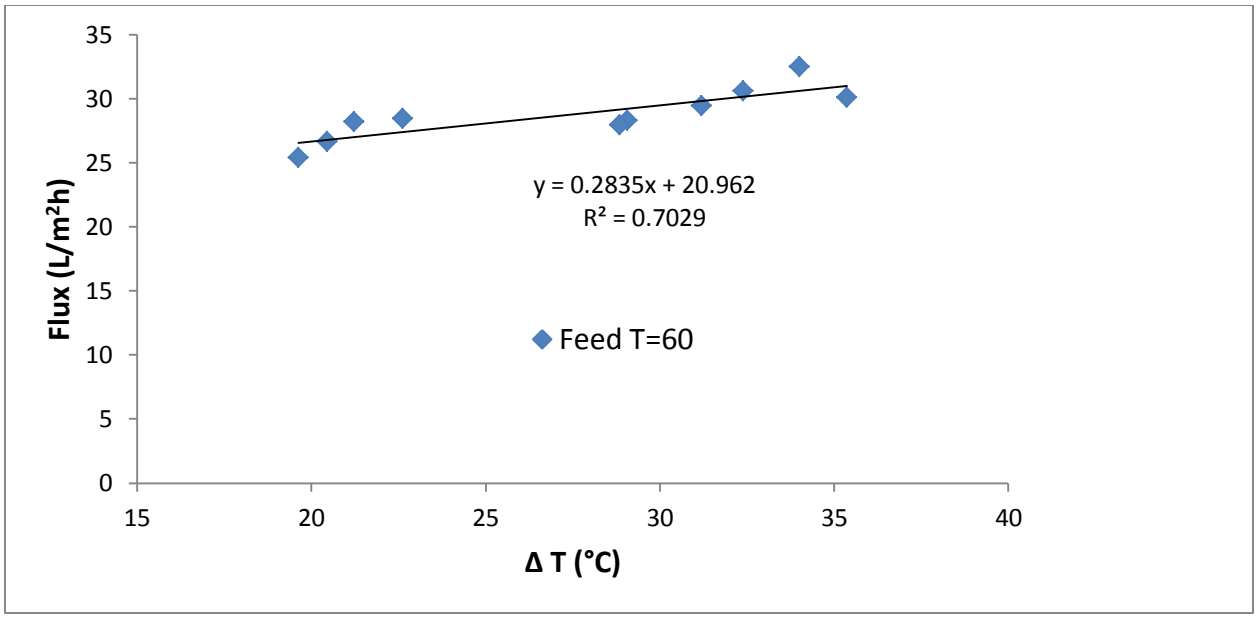

Figure 4.5 Averaged permeate flux and ΔT's for wastewater tests 2 and 3. Wastewater effluent feed solution, 0.22µ PTFE membrane, feed temperature of approximately 60°C, ΔT of 20- 35°C, and channel crossflow velocity of 0.24 m/s.

The NaCl feed solution results shown in Figure 4.4 represent data with an increase in ΔT by increasing the feed temperature. The wastewater feed solution results in Figure 4.4 show data points with an increase of ΔT established by decreasing the permeate temperature. Since tests represented in Figure 4.3 had increasing feed temperatures, it had a greater slope than Figure 4.4. It appears that the permeate temperature has less of an effect on the permeate flux than the feed temperature. A MD desalination study by Banat and Simandl in 1998 and by Matheswaren et al. in 2007 stated that the effect of the cold side temperature on the permeate flux can be neglected with a fixed hot side temperature. The effect of the cold side temperature is less important because of the low variation of vapor pressure at low temperatures (Banat and Samandl 1998, Matheswaren et al. 2007, Alkhundhiri et al. 2012).

4.3d Feed Temperature and Membrane Material and Pore Size

Feed temperatures of 40, 50, 60 and 70°C and their effect on permeate flux were investigated for each of the three membranes. The results for all three membranes are shown in Figure 4.6. The three membranes used were compared systematically with the NaCl test results and are shown in Figure 4.6.

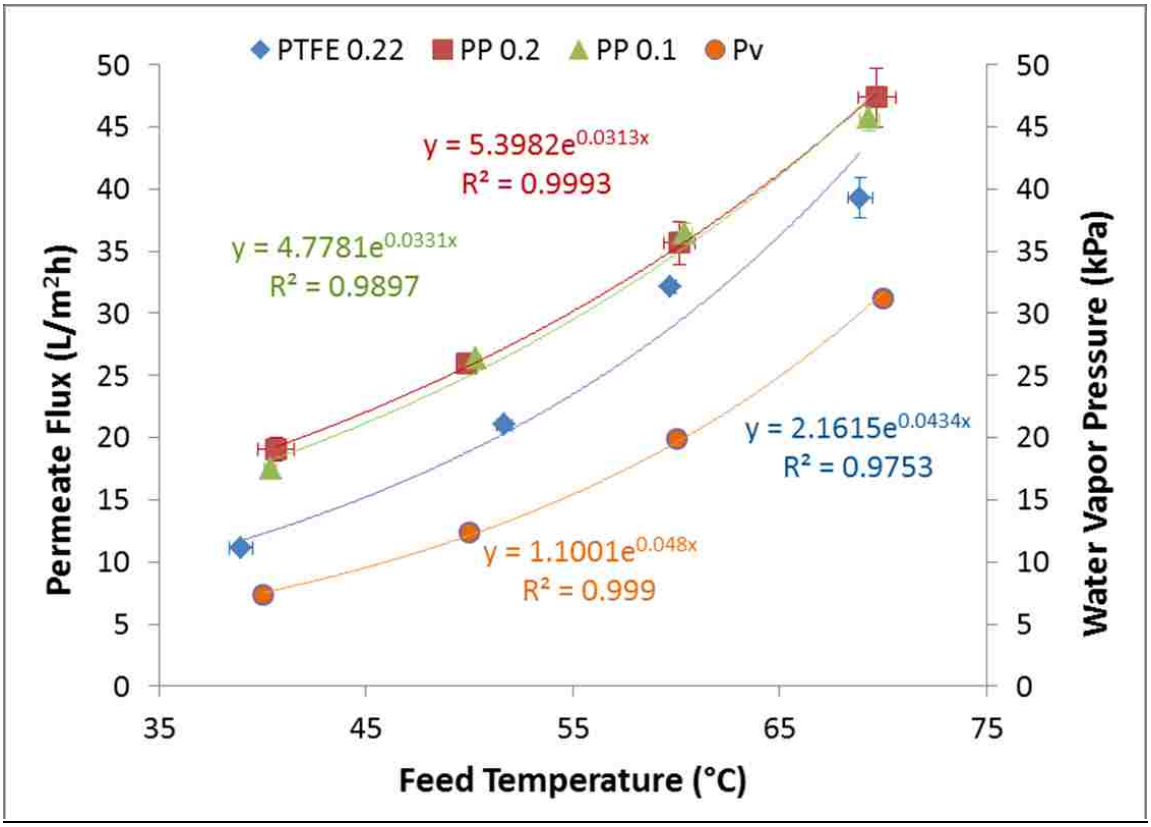

Figure 4.6 Running average permeate fluxes for corresponding feed temperatures for all membranes and feed temperatures of the NaCl tests at a constant ΔT (20°C). For the 0.22µm PTFE, 0.1µm PP, and 0.2µm PP membrane: 500 mg/L NaCl feed solution, feed temperatures of 40, 50, 60 and 70°C, ΔT of 20°C, and channel crossflow velocity of 0.24 m/s.

The permeate flux increased exponentially for all membranes as feed temperature increased. The flux results can be examined in part by referring Equation 4.4 to the

membrane trend equations shown in Figure 4.6. The y-axis in Figure 4.6 corresponds to the permeate flux *J*, which is dependent on ΔV_p which displayed an exponential dependence on temperature. The membrane distillation mass transfer coefficient, *C*, is dependent on the feed solution composition, temperature and membrane characteristics. Since the feed solution and temperature difference were the same for each test, the membrane characteristics were responsible for the variation between the results. Pore size, pore size distribution, tortuosity, thickness, and surface chemistry of the 0.2 μm PP membrane had the best results for this MD process and module with the highest *C* values shown in Table 4.2. This shows that the features of the PP material were better suited for this particular flat sheet DCMD process.

Table 4.2 Calculation of flux parameters *C* and *ΔV*

			J			*Vf*	*Vp*	*ΔV*	*C*
Variable	**Membrane**	**Feed Solution**	**Flux Avg. (L/m^{2}h)**	**Tf Avg.**	**Tp Avg**	**(kPa)**	**(kPa)**	**(kPa)**	**(L/m2h·kPa)**
T_f & Membrane	PTFE.22	500 mg/L NaCl	11.1	39.0	20.3	9.0	3.4	5.6	2.0
T_f & Membrane	PTFE.22	500 mg/L NaCl	21.0	51.7	30.9	18.3	5.8	12.5	1.7
T_f & Membrane	PTFE.22	500 mg/L NaCl	32.1	59.7	41.0	27.8	10.1	17.7	1.8
T_f & Membrane	PTFE.22	500 mg/L NaCl	39.3	68.9	50.7	42.9	17.4	25.6	1.5
T_f & Membrane	PP.2	500 mg/L NaCl	19.1	40.6	20.1	9.9	3.4	6.5	2.9
T_f & Membrane	PP.2	500 mg/L NaCl	26.0	49.9	30.1	16.6	5.5	11.0	2.4
T_f & Membrane	PP.2	500 mg/L NaCl	35.7	60.2	40.5	28.4	9.8	18.5	1.9
T_f & Membrane	PP.2	500 mg/L NaCl	47.4	69.7	50.0	44.5	16.7	27.8	1.7
T_f & Membrane	PP.1	500 mg/L NaCl	17.5	40.4	20.3	9.8	3.4	6.4	2.8
T_f & Membrane	PP.1	500 mg/L NaCl	26.4	50.3	30.2	17.0	5.6	11.4	2.3
T_f & Membrane	PP.1	500 mg/L NaCl	36.4	60.4	40.6	28.8	9.9	18.9	1.9
T_f & Membrane	PP.1	500 mg/L NaCl	45.7	69.3	50.1	43.7	16.8	26.9	1.7
Δ T									
20°C	PTFE.22	500 mg/L NaCl	11.13	39.0	20.3	9.0	3.4	5.6	2.0
25°C	PTFE.22	500 mg/L NaCl	18.5	45.0	20.2	12.7	3.4	9.3	2.0
30°C	PTFE.22	500 mg/L NaCl	23.4	52.4	23.5	19.0	4.0	15.1	1.6
Crossflow Velocity									
0.24 m/s	PTFE.22	500 mg/L NaCl	11.1	39.0	20.3	9.0	3.4	5.6	2.0
0.29 m/s	PTFE.22	500 mg/L NaCl	12.2	40.3	20.1	9.7	3.4	6.3	1.9
0.39 m/s	PTFE.22	500 mg/L NaCl	14.3	40.5	20.0	9.8	3.4	6.5	2.2
Feed Solution									
NaCl	PTFE.22	500 mg/L NaCl	11.1	39.0	20.3	9.0	3.4	5.6	2.0
WW	PTFE.22	WW Effluent	14.6	40.6	20.0	9.9	3.4	6.5	2.2
NaCl	PTFE.22	500 mg/L NaCl	18.5	59.7	41.0	27.7	10.1	17.6	1.0
WW	PTFE.22	WW Effluent	26.7	60.4	39.4	28.7	9.2	19.5	1.4
NaCl	PP.1	500 mg/L NaCl	17.5	40.4	20.3	9.8	3.4	6.4	2.7
WW	PP.1	WW Effluent	17.2	41.0	20.3	10.1	3.4	6.7	2.6

The exponential relationship between the feed temperature and permeate flux was supported by 51 studies reviewed by El-Bourawi et a.l in 2006 for various membranes and MD systems that investigated parameter effects on permeate flux. A summary of MD performance operational variables gathered from multiple published papers in El-Bourawi et al. 2006 indicated that in all MD configurations there is an exponential increase of the MD flux with the increase of the feed temperature. As discussed in section 4.1, the flux trend with respect to feed temperature is proportional to the vapor pressure inside the membrane pores. The exponential increase of the flux shows a direct relationship with the exponential vapor pressure increase, shown in Figure 5, as a

function of the feed solution temperature, which increases the transmembrane vapor pressure (i.e. the driving force) as all the other involved MD parameters are constant (El-Bourawi et al. 2006). The feed temperature results gives confirmation that the exponential flux trend holds true for this particular direct contact membrane distillation system. The qualitative exponential shape strength of this relationship varies among the different membranes, with the PP 0.2μm membrane having the strongest with an R^2 value of 0.999. This membrane material and pore size allowed the water vapor to travel across the membrane with the least resistance due to heat loss, concentration and temperature polarization, and fouling. The water molecules were allowed to turn into vapor at a rate most similar to the vapor pressure curve in Figure 5. This membrane also showed the highest of fluxes of the three. System efficiencies for each of the membranes are discussed in section 1f. Results from the three membranes are shown in Table 4.3 to compare the flux increases between each temperature and with respect to the baseline tests for each membrane. The 0.2μm PP membrane has the most consistent increases of flux from one temperature to the next. The other two show a decreasing fractional flux increase above 50°C.

Table 4.3 Membrane Material and Pore Size Feed Temperature Results

Feed Temperature and Membrane Type Effects on Flux				
Membrane	**Test**	**Flux (L/m^2h)**	**% of PTFE flux**	**% of PP 0.2 flux**
PTFE 0.22µm	Baseline	11.1	0	58
PP 0.2µm	Baseline	19	171	100
PP 0.1µm	Baseline	17.5	158	92
Membrane	**Feed Temp (°C)**	**Flux (L/m^2h)**	**% Increase from baseline flux**	**% Increase from previous flux**
PTFE 0.22µm	40	11.1	0	0
PTFE 0.22µm	50	21	89	89
PTFE 0.22µm	60	32.1	189	53
PTFE 0.22µm	70	40	260	25
PP 0.2µm	40	19	0	0
PP 0.2µm	50	26	37	37
PP 0.2µm	60	35.6	87	37
PP 0.2µm	70	47.3	149	33
PP 0.1µm	40	17.5	0	0
PP 0.1µm	50	26.4	51	51
PP 0.1µm	60	36.4	108	38
PP 0.1µm	70	45.7	161	26

4.3e Feed Solution

A 500 mg/L NaCl feed solution was prepared with DI water and NaCl. Wastewater effluent was collected from the ABCWUA Southside Reclamation Plant. The wastewater characteristics are shown in Table 3.10. Three tests from the NaCl and wastewater feed tests that had the same MD parameter settings were compared. Figure 4.7 and Figure 4.8 show results for the 0.22 µm PTFE membrane. Figure 4.7 shows results for a feed temperature of 40°C, ΔT of 20°C, and crossflow velocity of 0.24 m/s. Figure 4.8 shows results for a feed temperature of 60°C, ΔT of 20°C, and crossflow velocity of 0.24 m/s. Figure 4.9 shows results for the 0.1 µm PP membrane with a feed temperature of 40°C, ΔT of 20°C, and crossflow velocity of 0.24 m/s.

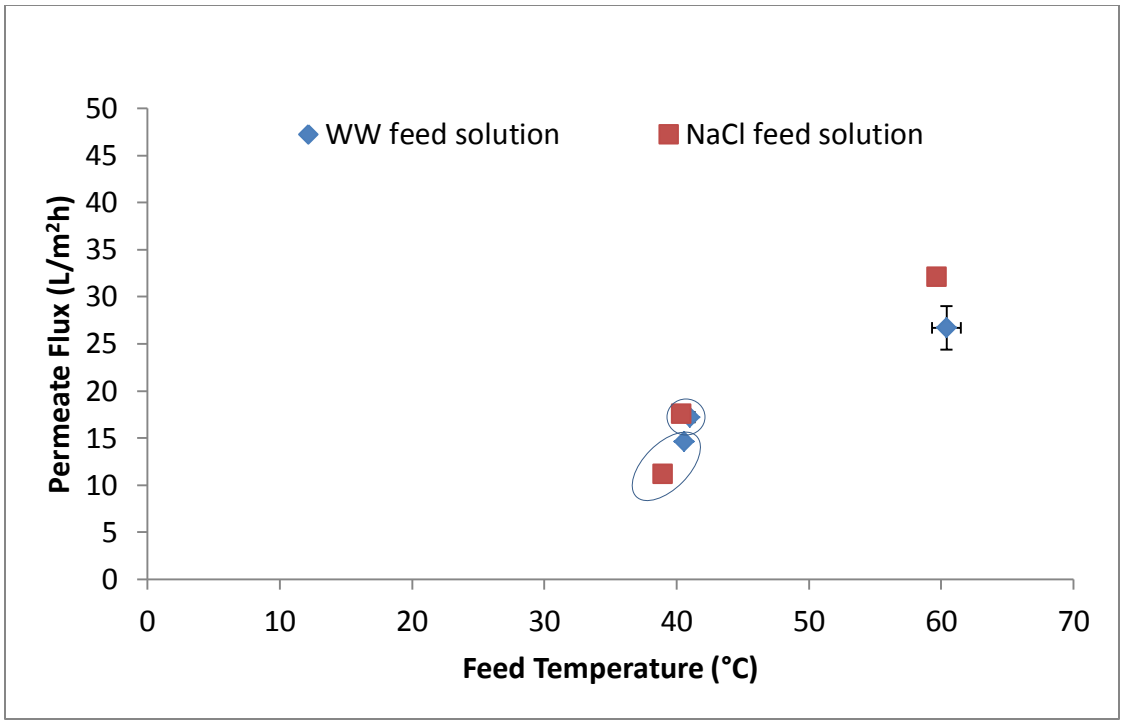

Figure 4.7 NaCl tests 1, 3 and 13 and wastewater effluent tests 1, 2, and 5. Wastewater effluent and NaCl feed solutions, 0.22 µm PTFE and 0.1 µm PP membrane, feed temperatures of 40 and 60°C, ΔT of 20°C, and channel crossflow velocity of 0.24 m/s. Error bars represent one standard deviation of the feed temperature and permeate flux.

The data points grouped at the lower end of the 40°C feed temperature represent NaCl test 1 and wastewater effluent test1, described in the experiment matrices in Table 3.1 and 3.2. These tests involved the 0.22µm PTFE membrane. The wastewater effluent appeared to have a 3.5 L/m^{2}h higher permeate flux, which is 32% greater than the NaCl flux, at a target feed temperature of 40°C, though the average feed temperature was about 1.5°C higher than the NaCl test (Figure 4.7). This is to be expected with the permeate flux increasing as temperature increases shown previously in Figure 4.6. The data points with a feed temperature of 60°C represent NaCl test 3 and wastewater effluent test 2. These tests also involved the 0.22µm PTFE membrane. The NaCl feed solution test gave

a 5.3 L/m^{2}h higher permeate flux , which is a 20% increase, than the wastewater effluent feed solution test at the target feed temperature of 60°C. Since the NaCl test had an average ΔT of 18.5°C and the wastewater feed test had an average ΔT of 20.9°. This difference in ΔT could explain the difference in flux since this pattern is not expected from previous results showing that a higher temperature produces a higher flux. The upper grouped data points within the 40°C feed temperature represent NaCl test 13 and wastewater effluent test 5. This test involved the 0.1μm PP membrane. The NaCl feed solution test produced about 0.3 L/m^{2}h higher flux, a 2% increase, on average than the wastewater effluent feed solution test. The test comparison in Figure 4.9 with feed temperature of 40°C had the only notable flux difference of 3.5 L/m^{2}h, which was likely due to the difference in ΔT. Therefore the feed solution composition type does not seem to have as great of an influence on the permeate flux than the membrane and pore size, especially at higher feed temperatures.

4.1f System Energy Efficiency

The energy efficiency of the system was calculated for each test. The average efficiencies for the NaCl feed tests and wastewater effluent tests are shown in Table 4.4. Figure 4.8 shows the efficiency results for the three membranes for the NaCl feed solution at the feed temperatures of 40, 50, 60, and 70°C using Equation 4.3.

Table 4.4 Energy Efficiency for NaCl and Wastewater Effluent Feed Tests

Test #	Feed Solution	Feed Temperature (°C)	Delta T (°C)	Crossflow Velocity (m/s)	Membrane Type	Pore Size (µm)	Average Permeate Flux (L/m^{2}h)	Average Energy Efficiency (%)
1	500 mg/L NaCl	40	20	0.24	PTFE	0.22	11.1	36
2	500 mg/L NaCl	50	20	0.24	PTFE	0.22	21	47
3	500 mg/L NaCl	60	20	0.24	PTFE	0.22	32.1	66
4	500 mg/L NaCl	70	20	0.24	PTFE	0.22	39.3	60
5	500 mg/L NaCl	50	30	0.24	PTFE	0.22	23.1	44
6	500 mg/L NaCl	45	15	0.24	PTFE	0.22	18.4	42
7	500 mg/L NaCl	40	20	0.29	PTFE	0.22	12.2	39
8	500 mg/L NaCl	40	20	0.39	PTFE	0.22	14.3	57
9	500 mg/L NaCl	40	20	0.24	PP	0.2	19	60
10	500 mg/L NaCl	50	20	0.24	PP	0.2	26	61
11	500 mg/L NaCl	60	20	0.24	PP	0.2	35.6	62
12	500 mg/L NaCl	70	20	0.24	PP	0.2	47.3	68
13	500 mg/L NaCl	40	20	0.24	PP	0.1	17.5	50
14	500 mg/L NaCl	50	20	0.24	PP	0.1	26.4	60
15	500 mg/L NaCl	60	20	0.24	PP	0.1	36.4	66
16	500 mg/L NaCl	70	20	0.24	PP	0.1	45.7	62
1	WW Effluent	40	20	0.24	PTFE	0.22	14.6	44
2	WW Effluent	60	20	0.24	PTFE	0.22	26.4	51
3	WW Effluent	60	40	0.24	PTFE	0.22	30.2	47
4	WW Effluent	40	20	0.39	PTFE	0.22	13.5	56
5	WW Effluent	40	20	0.24	PP	0.1	17.2	48
6	WW Effluent	40	20	0.24	PP	0.1	17.5	47
7	WW Effluent	40	20	0.29	PP	0.1	16.3	50
8	WW Effluent	40	20	0.24	PP	0.1	16.6	-

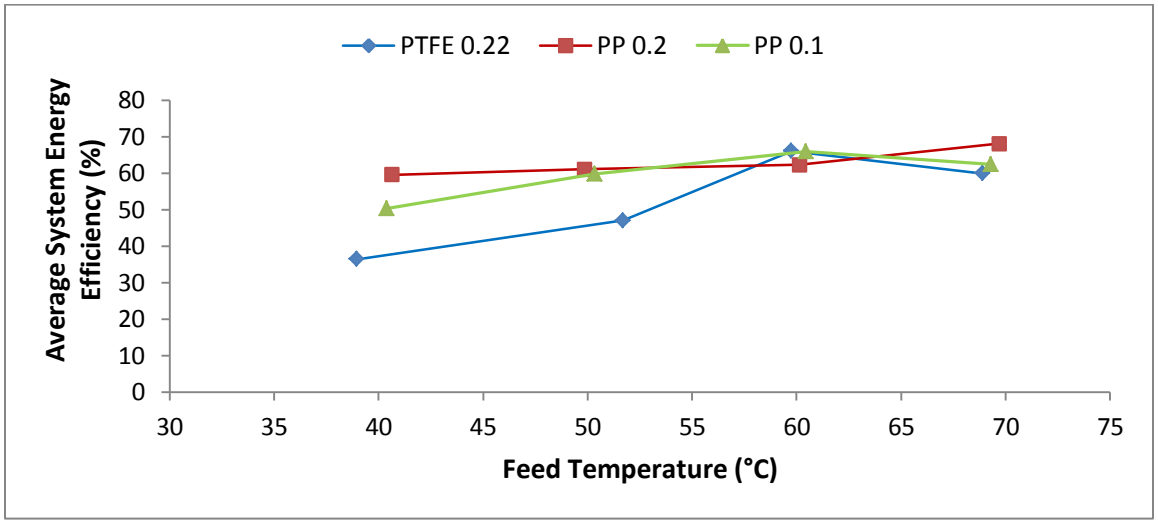

Figure 4.8 Average system efficiency for corresponding feed temperatures for all membranes with varying feed temperature tests. 500 mg/L NaCl feed solution, feed

temperatures of 40, 50, 60 and 70°C, ΔT of 20°C, and channel crossflow velocity of 0.24 m/s.

The 0.2 μm PP gave the highest average energy efficiencies and was the only membrane to have efficiencies consistently increase with increased feed temperature. At a feed temperature of 60°C, the 0.2 μm PP was only 0.3% less efficient than the other two membranes at that temperature. All membranes were subjected to the same system parameters to compare their results for increasing feed temperature and their efficiencies at these temperatures and the only difference was the membrane material and pore size. The PP membranes had higher fluxes for the majority of feed temperatures. The non-porous laminate on the PTFE could have resulted in lower fluxes. The 0.2 μm PP had mostly higher fluxes for the majority of the various feed temperatures, and more consistent increase in fluxes than the 0.1 μm PP. The difference between the PP membrane results could be due to the pore sizes and the difference in structure of the material. Since the 0.2 μm PP membrane was thicker and had the most uniform surface, it gave the highest fluxes, and had the majority of highest overall system efficiencies, and was selected for the membrane cleaning tests in phase three.

4.4 Treated Wastewater Fouling

Due to availability, the 0.1 μm PP was used for the wastewater fouling section. Wastewater test 6 and 8 were run with a feed temperature of 40°C, a ΔT of 20°C and crossflow velocity of 0.24 m/s. Test 6 was run continuously for over 26 hours without apparent flux decline. Test 8 was run continuously for over 40 hours, until the flux declined to zero. The results are shown for test 8 in Figure 4.9.

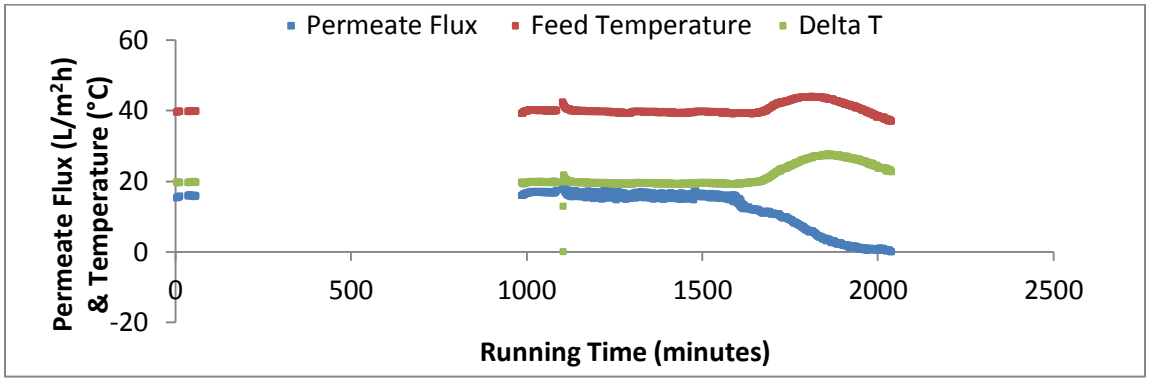

Figure 4.9 Wastewater effluent test 8. Wastewater effluent feed solution, 0.1 µm PP membrane, feed temperature of 40°C, ΔT of 20°C, and channel crossflow velocity of 0.24 m/s.

The permeate flux started to decline after approximately 26 hours and reached 0 after about 34 hours total. The feed temperature increased to about 4°C above the target feed temperature and then fell because of a heat exchanger low level fault alarm, but the flux had already started to decrease by then. SEM images of the membrane surface in contact with the permeate side and feed side are shown in Figure 4.10 and 4.11 respectively.

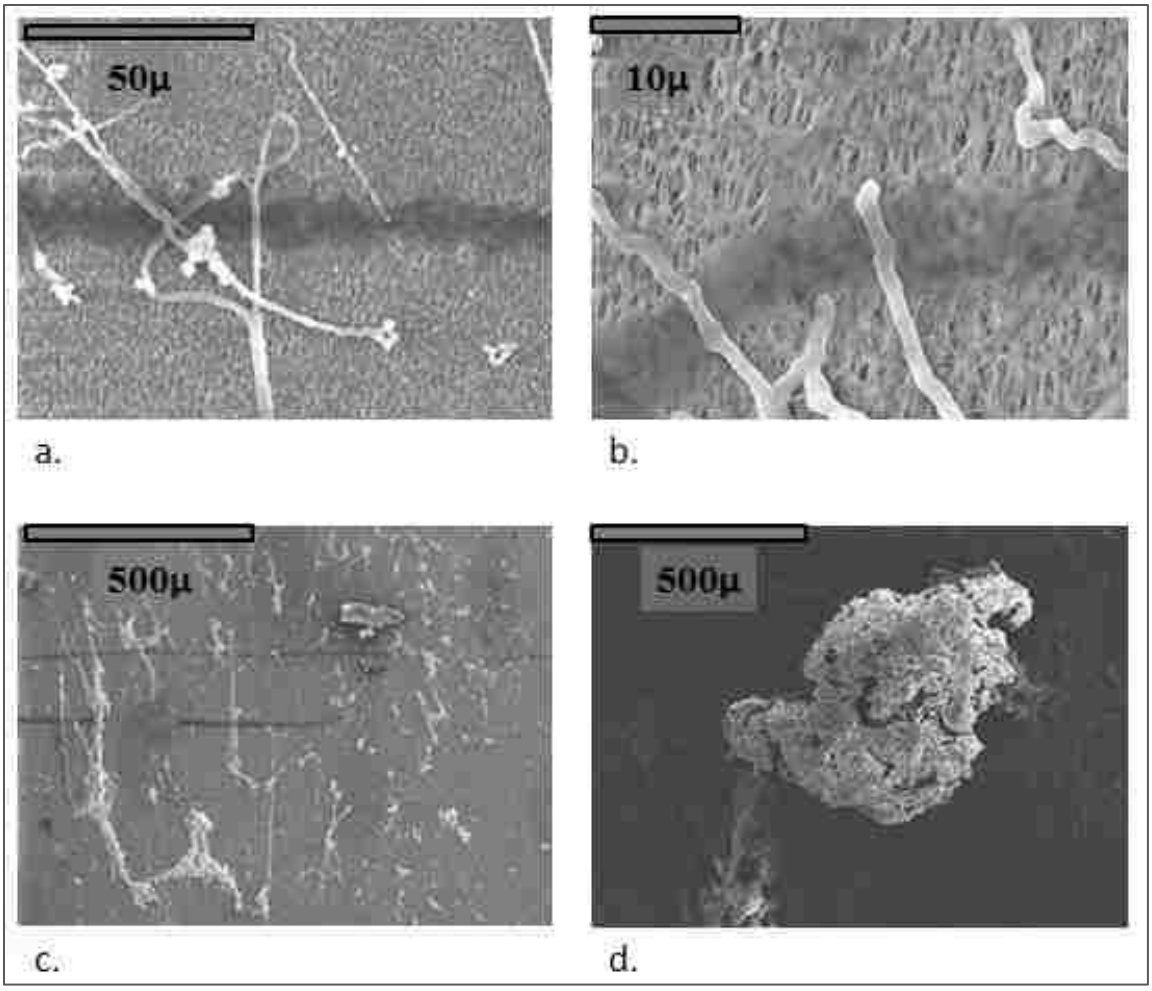

Figure 4.10 Wastewater effluent fouled 0.1 µm PP membrane surface in contact with permeate solution (a) magnified 1,000x (b) magnified 3,000x (c) magnified 100x (d) magnified 90x.

The side of the membrane in contact with the permeate was found to have bacteria, seen in Figure 4.10a-c, and a few silicon clumps from the degrading silicone based tubing, like the one shown in Figure 4.10d.

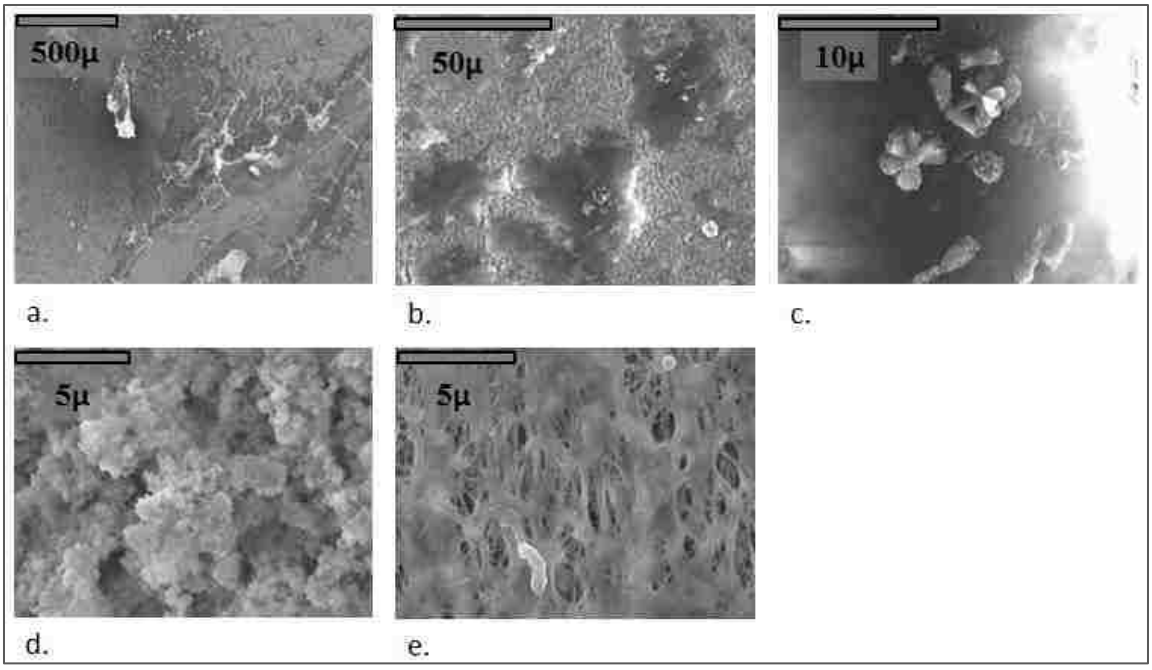

Figure 4.11 Wastewater effluent fouled 0.1 µm PP membrane surface in contact with the feed solution (a) magnified 65x, (b) magnified 1,000x, (c) magnified 5,000x (d) magnified 7,000x, and (e) magnified 17,000x.

Photos of the membrane surface in contact with the feed solution found various forms of fouling. Figure 4.13 identified the crystal structure in Figure 4.11c to be calcium carbonate. A cross section of the membrane with the feed side on top is shown in Figure 4.12. This SEM image shows that there was not any contaminant found inside the membrane matrix and fouling was restricted to the surface of the membrane.

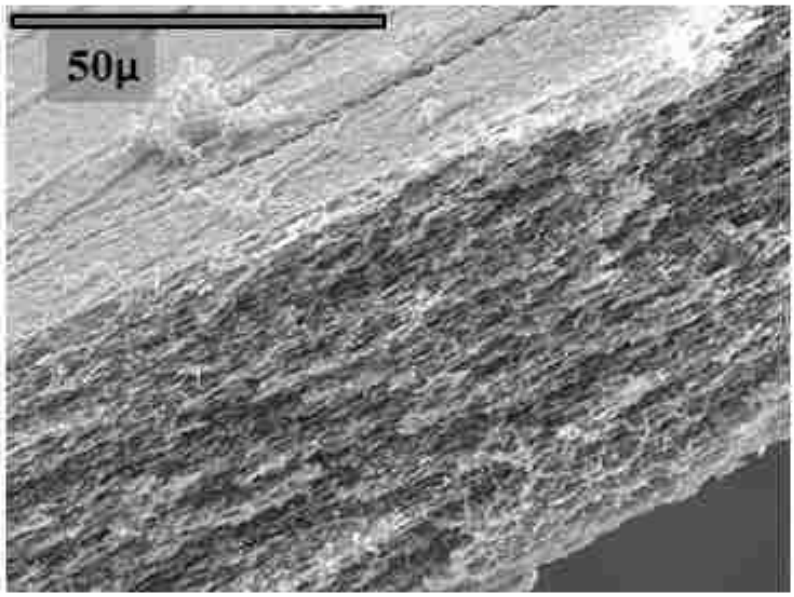

Figure 4.12 Cross-sectional SEM image of the wastewater effluent fouled 0.1 µm PP membrane magnified 1,000x.

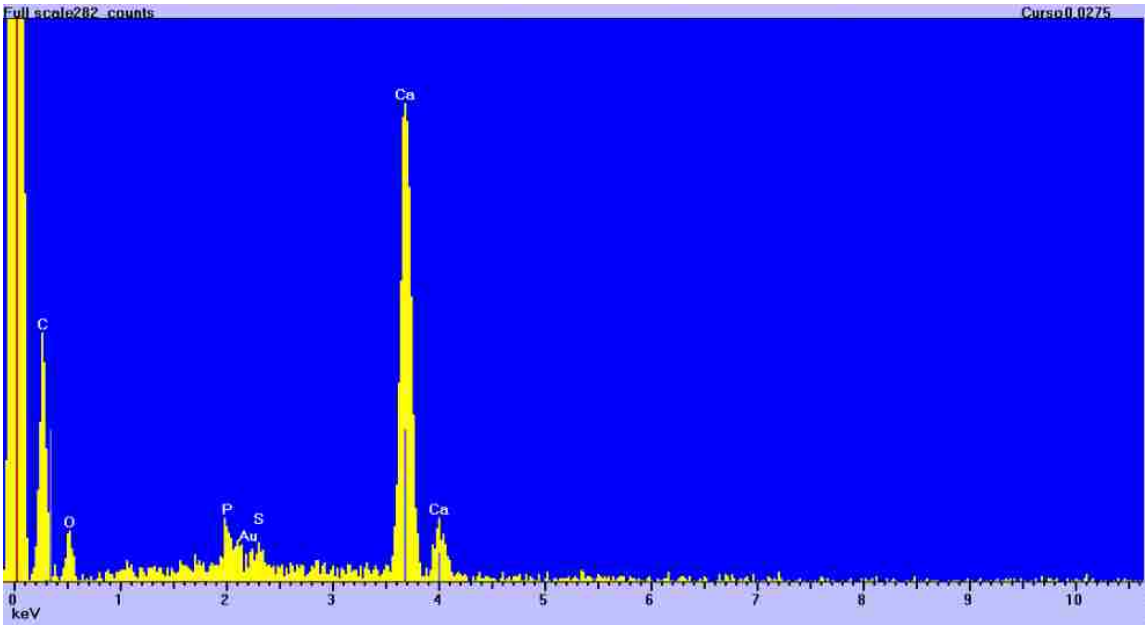

Figure 4.13 Radial crystal composition XRD analysis from 13(c).

It took over a day to foul the 0.1 μm PP membrane with the treated wastewater, thus parameters were adjusted for the membrane cleaning tests to promote fouling faster. Membrane fouling intensity was found to be limited by operating at a low feed temperature and a high flowrate (Gyra 2006). The rate of fouling increased when the TDS of the feed concentration increased (Tomaszwekska et al.)(Sakia et al)(Banat and Simaldi). Therefore, feed temperature was raised to 70°C and the crossflow velocity was reduced to 0.15 m/s. With a high feed temperature, a higher flux was established, causing the concentration of the feed solution to increase faster. An increase of feed concentration decreases the driving vapor pressure by restricting the path of the volatile molecules and by membrane fouling. An increase in feed concentration also increases the temperature polarization effect on the feed side, promoting fouling. A low crossflow velocity also increases temperature polarization, which can help promote fouling. Using a high feed temperature and low crossflow velocity, did cause flux decline due to membrane fouling to occur more rapidly and allowed for more time to be used for membrane cleaning investigation. The two cleaning tests results are shown in the next section.

4.5 Membrane Cleaning Tests

Two membrane cleaning tests were completed. The first test was used to develop the procedures and for parameter adjustment. Following the cleaning methods described in Chapter 3, this preliminary 0.2 μm PP membrane cleaning test involved running the treated wastewater feed solution at 70°C with a ΔT of 20°C at a crossflow velocity of 0.15 m/s. The EDTA cleaning solution was then circulated though the feed side for 15 minutes with the same temperature and velocity parameters. Wastewater effluent was run

through the feed side again to establish a flux recovery. The initial flux was about 47 L/m^2h and declined by 88% over a period of 4.6 hours. After a chemical membrane cleaning of 2mM EDTA (pH 11) at 70°C for 15 minutes, a 91% flux recovery to 43 L/m^2h was observed. These results are shown in Figure 4.14.

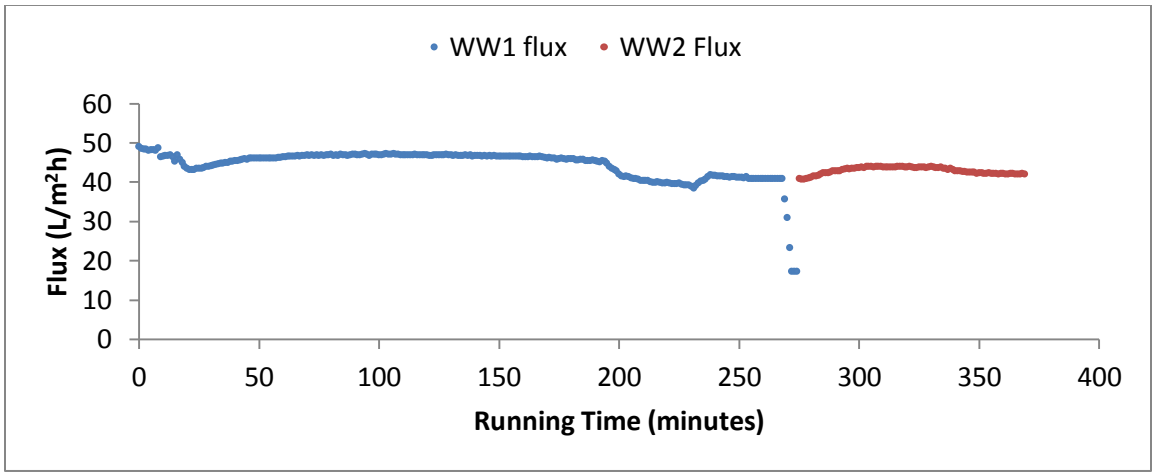

Figure 4.14 Membrane cleaning shakedown test results. WW1 represents the flux from the first wastewater feed before the clean, and WW2 is the flux recorded after a second wastewater feed.

This cleaning restored permeate flux back to 92% of the initial flux. However, the Tygon tubing underwent a minor chemical change indicated by a cloudy appearance, and the permeate samples indicated contaminant breakthrough. Pre-cleaning permeate had a conductivity value of 4µS/cm and 17µS/cm after cleaning. These results are shown in Table 4.5. The conductivity was 4.25µS before cleaning and 17.6µS post cleaning which suggests contaminant passage through the membrane. The 4.25µS conductivity of the pre-cleaning sample inducated a contamination of some sort that was most likely due to a previous test membrane tare that allowed wastewater effluent to fill the permeate loop. The post-cleaning permeate sample conductivity value was substantially higher,

suggesting that the EDTA with a pH of 11 at 70°C was in some way destructive to the membrane. The membrane was subsequently replaced and the EDTA temperature was reduced to 26°C and the cleaning time was increased to 30 minutes for the rest of the experiments. The crossflow velocities were also reduced slightly to 0.125m/s for operational preference.

Table 4.5 Conductivity and pH of Membrane Cleaning Test 1 Samples

Sample	Description	Conductivity (µS/cm)	pH
WW1	Initial Wastewater feed	920.9	7.01
WW2	Second wastewater feed	854.9	8.46
DI	Initial DI water in the permeate loop	1.8	5.5
Permeate 1	Permeate after 50% flux decline	4.25	6.25
Permeate 2	permeate after second wastewater effluent	17.6	6.58

The permeate conductivity increased by 2.4µS/cm after the flux decline and 15.8 µS/cm after the membrane cleaning. This means that an organic or non-organic was contaminating the permeate flux. Because of this conductivity increase in the permeate measurement, the cleaning procedure was altered for the second test. The temperature limit for the Tygon tubing was 74°C. The 2mM EDTA with pH of eleven had a 'B' rating for the tubing, meaning that the chemical attributes were fairly unlikely to interact with the tubing material in an adverse way. Since the high pH solution was running near the upper temperature limit, the cleaning solution temperature was reduced to 26°C to ensure tubing functionality. The cleaning time was increased to 30 minutes to ensure thorough

cleaning. A study on organic fouled RO membranes showed that decreasing the 0.5mM EDTA (pH 11) chemical cleaning solution temperature decreased the cleaning efficiency dramatically (Ang et al. 2006). This study also showed that increasing the cleaning time of a 0.5mM EDTA (pH 11) cleaning solution from 15 to 60 minutes, about doubled the cleaning efficiency.

SEM images of the membrane surfaces in contact with permeate and feed solutions after the second wastewater effluent feed are shown in Figure 4.15. These images show that both membrane surfaces were fairly clean except for a foul patch shown in Figure 4.15g.

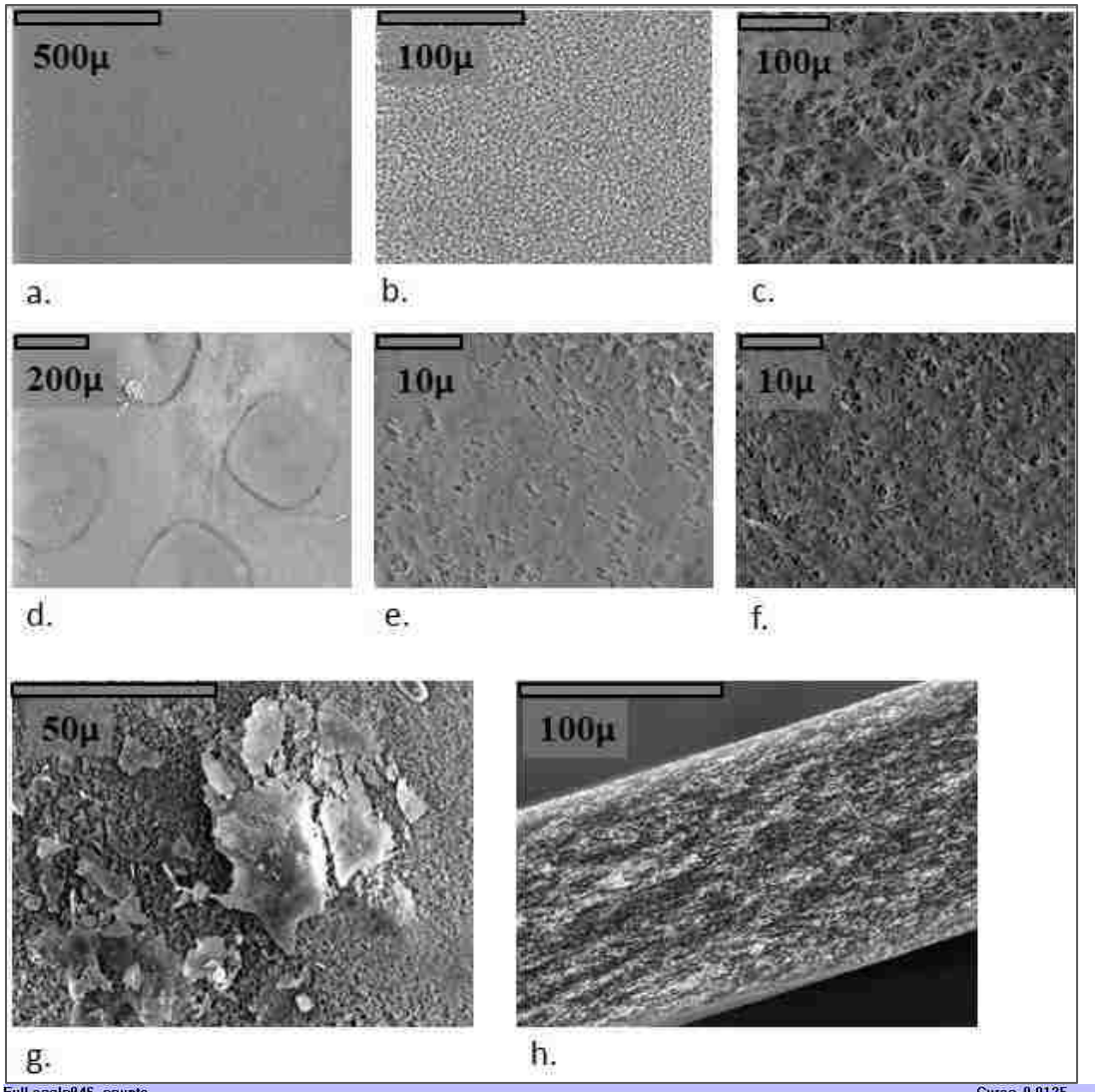
500µ
100µ
100µ
a.
b.
c.
200µ
10µ
10µ
d.
e.
f.
50µ
100µ
g.
h.

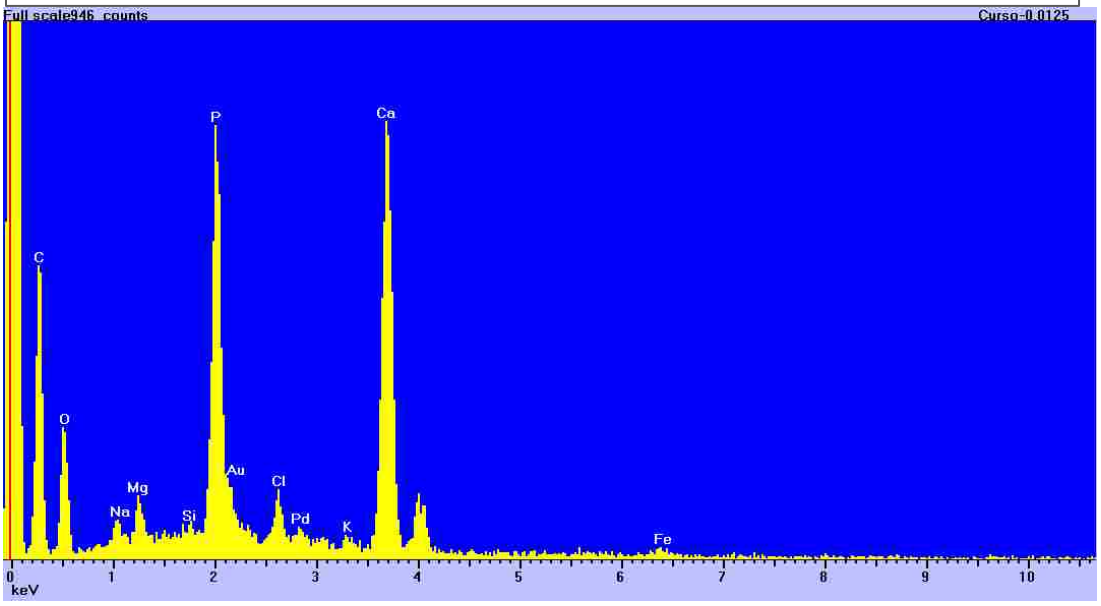
Full scale946 counts
Curso=0.0125
C
O
Na
Mg
Si
P
Au
Cl
Pd
K
Ca
Fe
0
1
2
3
4
5
6
7
8
9
10
keV

i.

Figure 4.15 Images and XRD analysis of the 0.2 μm PP for the shakedown membrane cleaning test. Membrane surface in contact with the permeate magnified 100x (a), 500x (b), and 3,000x (c). Membrane surface in contact with the wastewater effluent magnified 100x (d), on the pattern mark 3,000x(e), inside the pattern mark 3,000x (f), the membrane cross section magnified 500x (h), on a fouling cluster 1,000x (g), and the constituent composition XRD analysis (i).

The membrane surface in contact with the permeate solution appeared clean. The appearance of the feed side of the membrane changed as it can be observed when comparing Figure 4.1b with Figure 4.15d. Figure 4.15g shows a slight buildup on the feed membrane surface. Figure 4.15i identified this substance as calcium phosphate. This is a common membrane fouling constituent due to wastewater. Cells and biofilm composed mainly of carbon were seen in 4.15f. The cross section of the membrane image in 4.15h suggests that the pores were not clogged wXRDhich means the contaminant passage was likely do to pore wetting.

Since the chemical solution pH damaged the tubing, it could have also damaged the membrane to allow for pore wetting during the second wastewater feed solution. Reducing the cleaning solution temperature in the second test seems to have prevented or delayed any membrane damage to allow constituent passage, if it indeed was from the cleaning solution. A single membrane was able to undergo two membrane cleanings before contaminants were detected in the permeate. Test two results are shown in Figure 4.16 and Table 4.6 below. SEM images and XRD analysis summaries of the membrane surface, cross section, and fouling contaminates present after the third cleaning are shown in Figure 4.17.

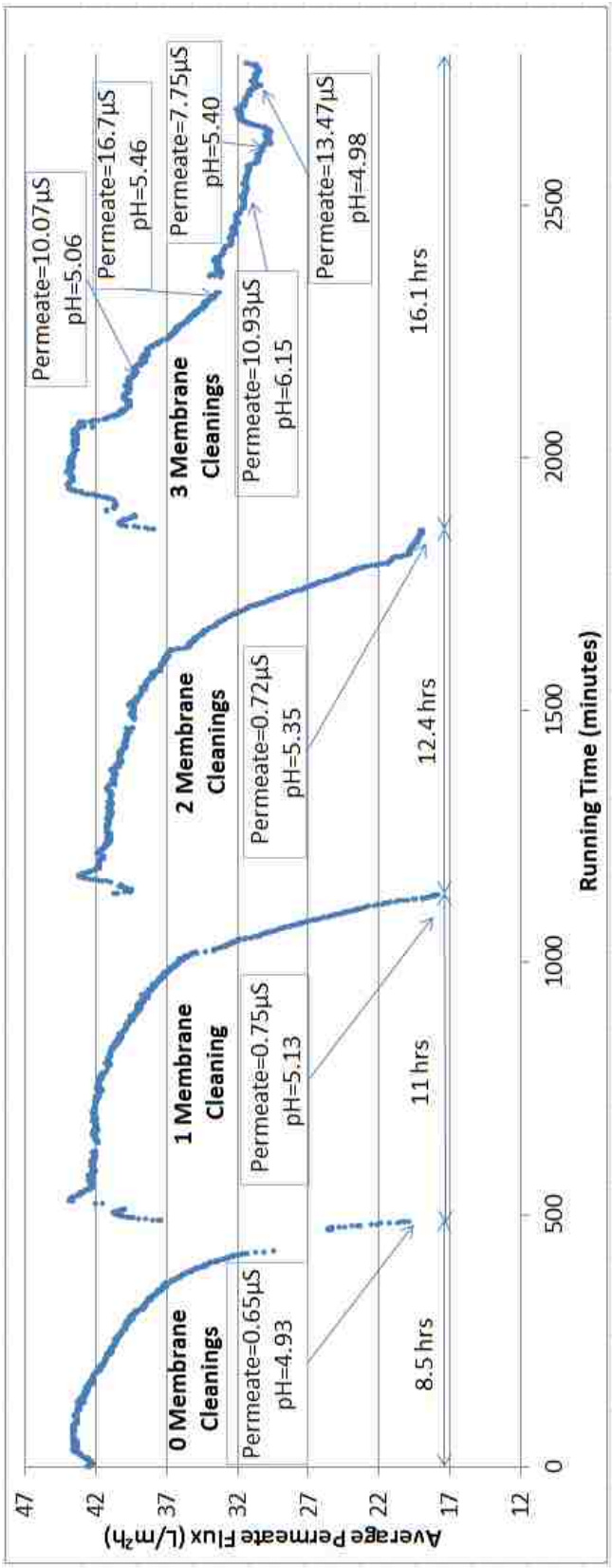

Figure 4.16 0.2 µm PP membrane cleaning test results.

Table 4.6 Conductivity and pH of Membrane Cleaning Test 2 Samples

Sample	Description	Conductivity (µS/cm)	pH
2PP.2MCWW1a Feed	Initial Wastewater feed	920.9	7.01
2PP.2MCWW1b Feed	WW1 after membrane fouled (concentrated)	1454	8.83
2PP.2MCWW1 Permeate	Permeate after WW1, no membrane cleaning	0.945	5.33
2PP.2MCWW2a Feed	Fresh WW feed after 1st membrane cleaning	926.4	6.4
2PP.2MCWW2b Feed	concentrated WW2	1712	-
2PP.2MCWW2 Permeate	Permeate after 1 membrane cleaning and fresh WW2 feed	0.87	5.13
2PP.2MCWW3a Feed	Fresh WW feed after 2nd membrane cleaning	918.5	7.02
2PP.2MCWW3b Feed	concentrated WW3	1723	8.75
2PP.2MCWW3 Permeate	Permeate after 2 membrane cleanings	0.72	5.25
2PP.2MC WW4a feed	Fresh WW feed after 3rd cleaning	929.6	6.88
2PP.2MC WW4b feed	Concentrated WW4	1851	8.77
2PP.2MCWW4a permeate	Permeate after 3 membrane cleanings	1.31	5.39
2PP.2MCWW4b permeate	Permeate after 3 membrane cleanings	2.6	5.46
2PP.2MCWW4c permeate	Permeate after 3 membrane cleanings	10.07	5.06
2PP.2MCWW4d permeate	Permeate after 3 membrane cleanings	16.7	5.46
2PP.2MCWW4e permeate	Permeate after 3 membrane cleanings	37.81	4.96
DI water	DI water in permeate loop	1.231	5.52
DI water	DI water in permeate loop	0.76	5.6
DI water	DI water in permeate loop	0.782	5.51

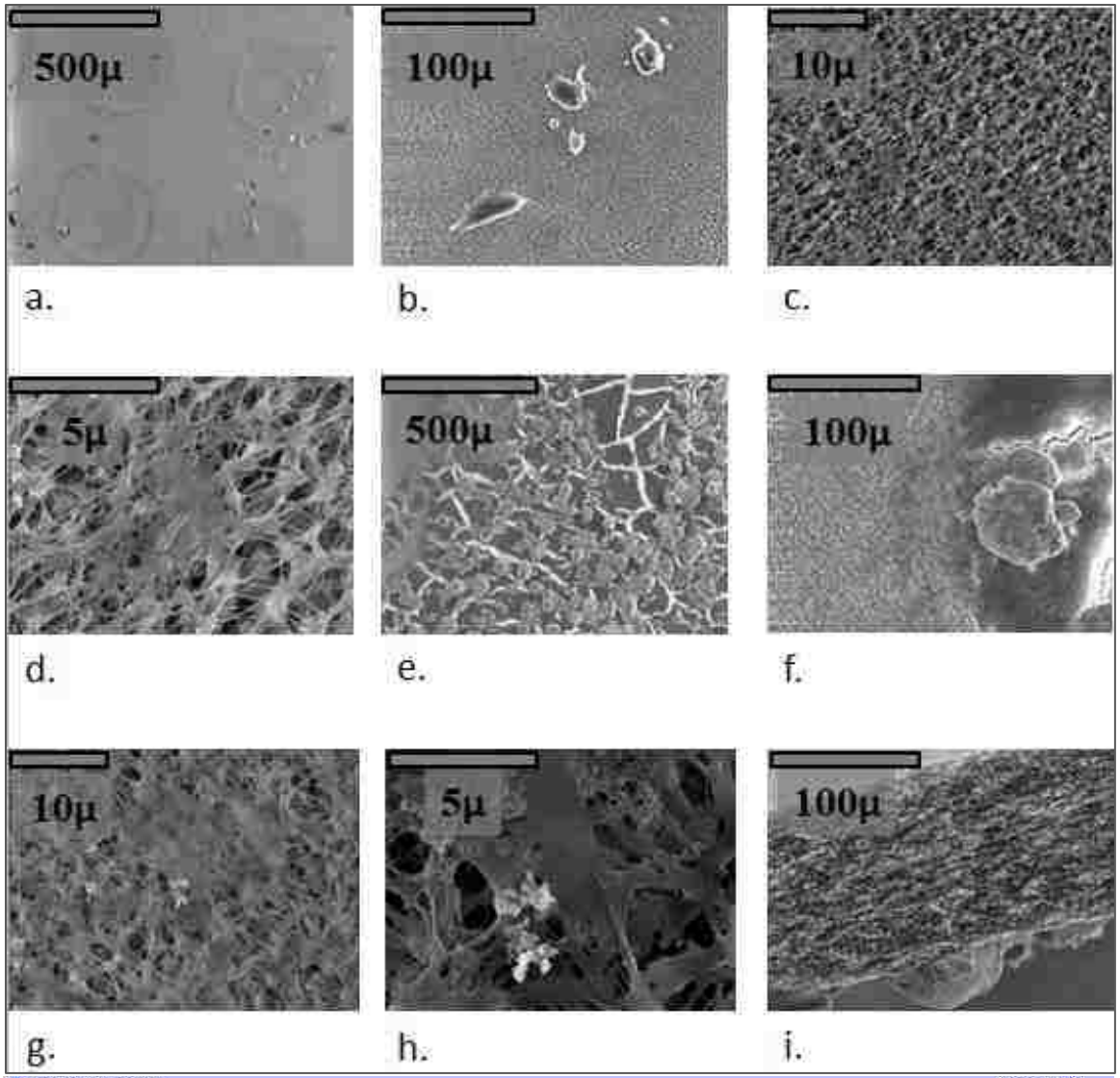
500µ
100µ
10µ
a.
b.
c.
5µ
500µ
100µ
d.
e.
f.
10µ
5µ
100µ
g.
h.
i.

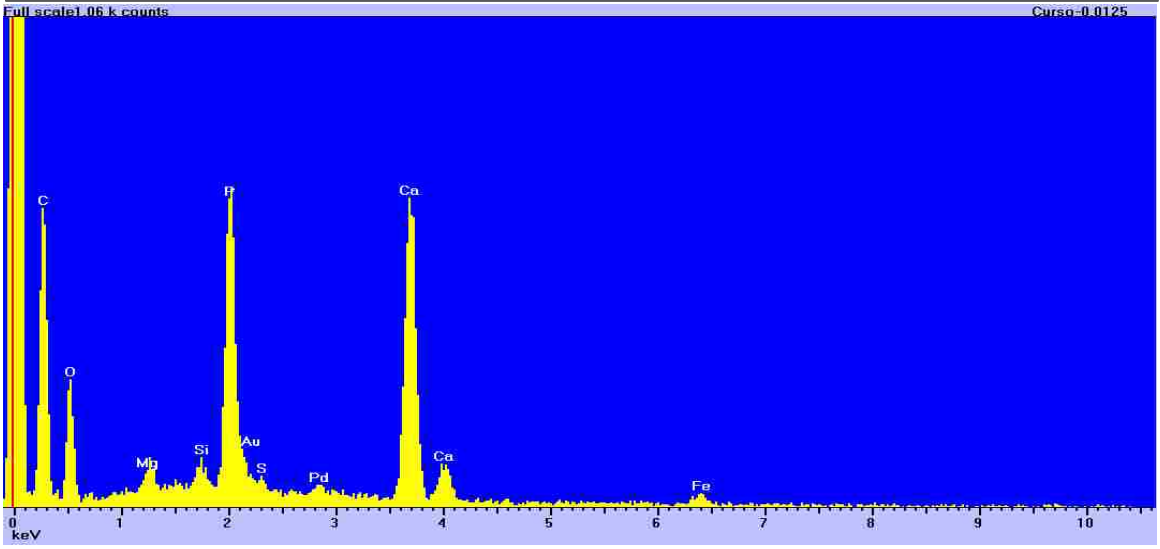
Full scale1.06 k counts
Curso=0.0125
C
O
Mg
Si
P
S
Au
Pd
Ca
Ca
Fe
0
keV
1
2
3
4
5
6
7
8
9
10

(j)

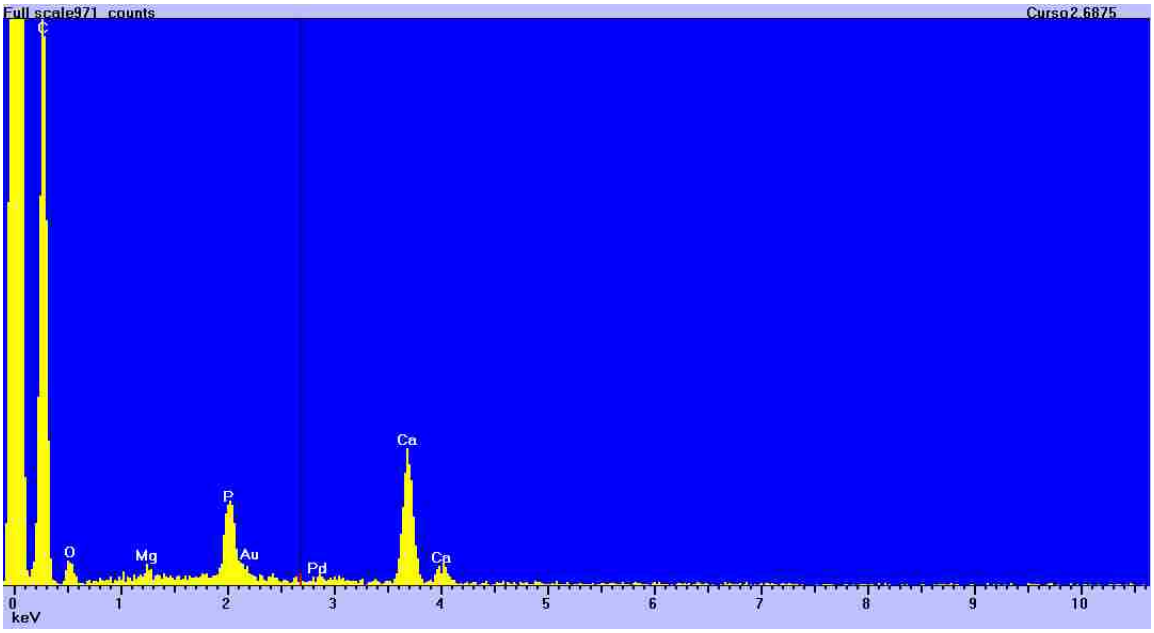

(k)

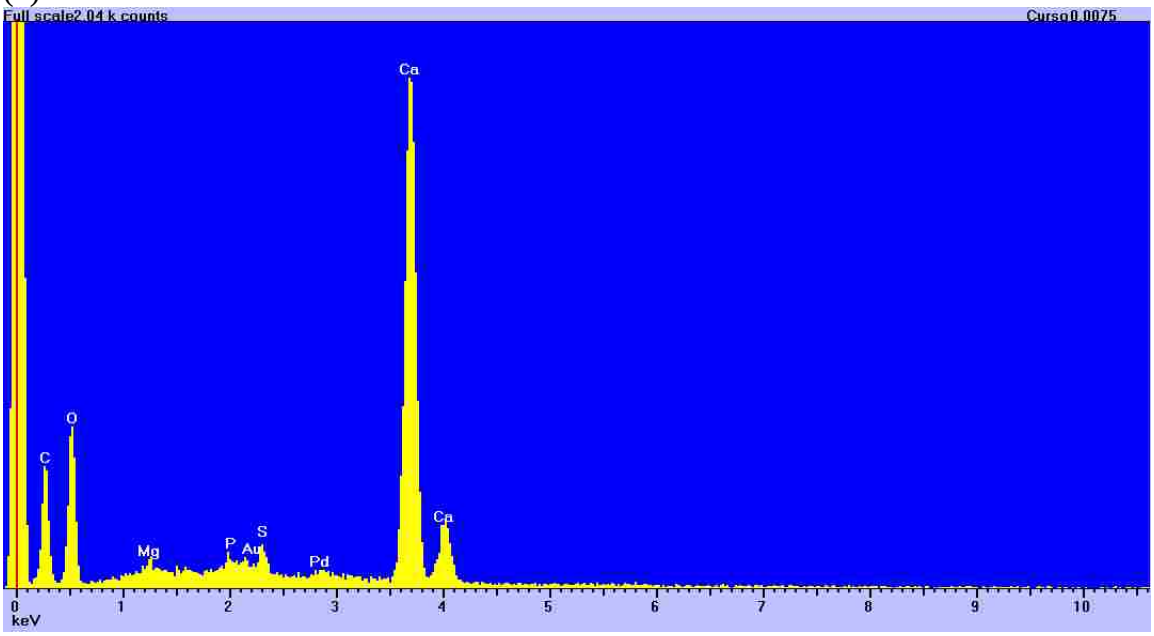

(l)

Figure 4.17 SEM images and XRD analysis of the 0.2µm PP after three membrane cleanings. Membrane surface in contact with the permeate magnified 100x (a), 500x (b), 3,000x (c), and 10,000x (d). Membrane surface in contact with the wastewater effluent magnified 100x (d), 500x (e), 3,000x (f), and 10,000x (g). The membrane cross section magnified 500x (i). Constituent composition XRD analysis results of the solids found in 20e and 20f (j), the cracked surface found in 20e (k), and the clusters found in 61g and 20h (l).

The initial average flux of a new 0.2 μm PP membrane with the wastewater effluent feed solution was 43.5 L/m^{2}h and was declined to 18.2 L/m^{2}h after about 8.5 hours, a 58% decrease. After the first membrane cleaning, a flux of 42.5 L/m^{2}h was observed, resulting in a 98% recovery of the initial flux. The membrane was then fouled with a flux decline of 58% down to 17.7 L/m^{2}h over 11 hours. When a second membrane cleaning procedure was done, the permeate flux was 41.6 L/m^{2}h resulting in a 96% recovery. The DCMD system continued to operate until the permeate flux again declined to 19.2 L/m^{2}h and a third membrane cleaning was performed. The flux established had a range of 40.4 L/m^{2}h-43.6 L/m^{2}h (93-98% recovery) but had contaminant detected by the conductivity measurement in the permeate samples. The increase in conductivity in the samples shown in Table 4, represent some sort of organic contamination in the DI water before filling the permeate loop. The contamination could be from the DI water source, the beaker used to transfer the DI water, or from the sample bottle.

The membrane surface in contact with the permeate side seemed to be relatively clean compared to a new membrane. The foulant shown in Figure 4.179b was identified as calcium carbonate. The cracked substance which covered nearly the whole membrane in Figure 4.17e was identified in the EDS analysis (Figure 4.17k) as calcium phosphate. The light colored clumps in Figure 4.17g and Figure 4.17h contained various levels of carbon indicating that they were cells of some sort. The membrane surface in contact with the permeate solution had a trace of biofilm on it as seen in Figure 4.17c. The cross section shows a fouling layer that was shown to be as thick as 32μm. The inside of the pores of

the cross section appear to be clean, so fouling likely caused pore wetting, allowing wastewater effluent constituents to break through after the third cleaning.

Chapter 5. Conclusions

A laboratory scale DCMD system was constructed to produce a clean water permeate flux. This study presents findings about the system's functionality, parameter values, effects of membrane fouling by treated wastewater, and the effectiveness of a membrane chemical cleaning process. Testing was done in three phases. The first tests involved running DI water in the feed and permeate loop to establish system functionality including elimination of leaks and bubbles, and establishment of a permeate flux. The first sets of tests also involved running a 500 mg/L NaCl solution in the feed loop to determine the effects of system parameters such as, feed temperature, transmembrane temperature gradient (ΔT), channel crossflow velocity, and membrane type on the system's permeate flux, contaminant percent rejection system and energy use efficiency. Next, wastewater effluent from the SWRP was used as the feed solution to evaluate the effects of the treated wastewater on the membrane and permeate flux. Lastly, a chemical cleaning solution process was studied to determine the effectiveness for permeate flux recovery. One chemical cleaning shakedown test was performed to fine tune the process. A second chemical cleaning test consisted of three series of cleanings, in which two were successful for recovering 96% of the original flux with continual clean water production. After the third cleaning solution, contaminants were detected in the permeate flux samples. The rest of this chapter covers the conclusions for each phase, and how to potentially apply the results, and future work recommendations for this research area.

5.1 Permeate Flux

Phase one testing investigated the effect of feed temperature, Δ T, crossflow velocity, feed solution type and membrane type on the system reliability, productivity, and efficiency. Table 5.1 summarizes the results from phase one and two testing for the 0.22μm PTFE, 0.2 μm, and 0.1 μm PP flat sheet membranes used. The permeate fluxes produced by this particular DCMD system were similar, if not mostly higher than permeate flux ranges compared to other systems reported by Alkudhiri et al in 2012, seen in Table 5.1 and 5.2.

Table 5.1 System parameter and permeate flux reports for various MD systems (Alkhundhiri et al. 2012)

Ref	MD type	Membrane type	Pore size (μm)	Solution	Feed velocity (m/s)	T_f (°C)	Permeate kg/m² h
[5]	AGMD	PVDF	0.45	Artificial seawater	5.5 l/min	40–70	≈1–7
[50]	DCMD	PVDF	0.22	Pure water	0.1	40–70	≈3.6–16.2
[113]	DCMD	PTFE	0.2	NaCl (2 mol/l)	16 cm^3/s	17.5–31	≈2.88–25.2
[44]	DCMD	PTFE	0.2	Pure water	–	40–70	≈5.8–18.7
[63]	DCMD	PVDF	0.4	Sugar	0.45	61–81	≈18–38
[65]	DCMD	PVDF	0.4	Pure water	0.145	36–66	≈5.4–36
				NaCl (24.6 wt.%)	0.145	43–68	≈6.1–28.8
[24]	VND	3MC	0.51	Pure water	–	30–75	≈0.8–8.8 mol/m^2s
[41]	DCMD	PVDF	0.22	Pure water	0.23	40–70	≈7–33 l/m^2h
[68]	SGMD	PTFE	0.45	Pure water	0.15	40–70	≈4.3–16.2
[15]	DCMD	PVDF	0.11	Orange juice	2.5 kg/min	25–45	30×10^3–108×10^3
[14]	DCMD	PTFE	0.2	NaC l (5%)	3.3 l/min	5–45	1–42
[14]	AGMD	PTFE	0.2	NaC l (3%)	3.3 l/min	5–45	0.5–6

Table 5.2 More system parameter and permeate flux reports for various MD systems (Alkhundhiri et al. 2012)

Ref	MD type	Membrane type	Pore size (μm)	Solution	Concentration g/l	T_f (°C)	Permeate kg/m² h
[6]	AGMD	PVDF	0.22	Methanol/water	≈30–200	50	≈3.9–4.6
				Ethanol/water	≈30–150		≈3.95–4.9
				Isopropanol/water	≈10–95		≈4.0–5.0
[113]	DCMD	PTFE	0.2	NaCl	0–116.8	31	≈12.4–25.2
[63]	DCMD	PVDF	0.4	NaCl	0–5290	81	≈44–63
[65]	DCMD	PVDF	0.22	NaCl	0–24.6 wt.%	68	≈16–28.8
[120]	AGMD	PTFE	0.22	HNO_3	2–6 M	80	≈0.9–2.1 l/m^2h
[120]	VMD	PP	0.2	NaCl	100–300	55	10.7–7.0

Taking into consideration the different membranes, pore sizes, MD configurations and feed solution differences, the fluxes produced by the constructed laboratory DCMD system used for this research are relatively high compared to that previously reported. The DCMD design could have been a very efficient design, especially with the use of insulation on the feed tank and all tubing. Using small crossflow channels with net

spacers inside probably allowed for much less temperature polarization, allowing for greater water mass transfer, than other designs that were used. The fluxes are also comparable to RO's typical flux range of 0-50 L/m^2h.

5.2 Contaminant Rejection

An initial contaminant rejection percentage was calculated for the first 500mg/L NaCl test with the 0.22 μm PTFE membrane. Since the initial conductivity of the permeate loop was higher than the permeate sample, the permeate could have been degraded by mixing with contaminated the DI water initially in the loop. A rejection >99.7% was achieved, shown in Table 5.3. The permeate loop quality was improved by about 16% from its initial quality and is unknown if it would have continued to improve if the system was run for a longer time. Phase three further investigated contaminant rejection during the membrane cleaning tests by measuring pH, and conductivity of the permeate samples.

Table 5.3 Contaminant Rejection Example

Test	Sample	Conductivity, σ (μS/cm)	Temperature (°C)
1NaClPTFE0.22	Permeate DI	3.21	20.9
	Feed Solution	895	24.1
	Permeate	2.69	21.8

Phase two showed that membrane fouling from treated wastewater was able to completely stop the permeate flux in about 34 hours, using a PP0.1 membrane at a feed temperature of 40°C. SEM imagery of the fouled membrane surfaces showed fouling that consisted of bacteria, biofilm, calcium carbonate, and a silica-carbon substance. The silica substance was suspected to be from silicon based tubing that was used, which was greatly reduced when tygon tubing was used as a replacement. The other constituents are typical fouling characteristics from wastewater. These results gave a time frame and confirmed that a membrane chemical cleaning process could be evaluated in phase three.

5.3 Membrane cleaning flux recovery and contaminant rejection

Phase three used the PP0.2 membrane for its MD feed solution selectivity properties, high permeate flux and energy efficiency to investigate a membrane cleaning solution test. The cleaning solution used was 2mM EDTA (pH 11) to clean the feed loop after running treated wastewater through it an fouling the membrane to reach a flux decline of about 54-58%. The cleaning solution recovered the flux after three sequential cleanings by 97.7, 95.6, and 92.7-98% of the initial flux respectively. The system was able to constantly exclude constituents from the feed solution in the permeate flux until after the third membrane cleaning. Before any membrane cleanings and after 2 cleanings the permeate conductivity results ranged from 0.7-0.9µs/cm. After the third membrane cleaning, the permeate conductivity was measuring over time from 1.31-37.8µS/cm. Organic contaminants were detected in the permeate samples, but whether or not organics were sourced from the permeate, is obscured. The constituents could include chloride, nitrate, sulfate, phosphate, or sodium, magnesium, calcium, iron, or aluminum. Based on

the characteristics of the wastewater effluent, with an average Nitrogen, Ammonia total (as N) of 0.3 mg/L, TSS of 9.7 mg/L, cBOD of 3 mg/L, Nitrate of 8.7 mg/L, TIN of 9 mg/L, and alkalinity of 105.3 mg/L (as CaCO3) it can be concluded that a number of these constituents could have breached the membrane pores.

5.4 Summary and Recommendations

Results from this study help to give DCMD potential to becoming a large scale wastewater reuse application option. This configuration displayed success in removing a high percentage of contaminant removal from salinized and treated wastewater solutions. The EDTA chemical membrane cleaning process was successful in recovering permeate flux while ensuring clean water production for two cycles. This helps implement a DCMD membrane cleaning option that could reduce membrane replacement frequency. The chemical cleaning process studied was in-situ and simple, requiring low amounts of maintenance and operation time. Results indicated that a high membrane cleaning efficiency for DCMD can be attained at a low temperature, with little down time. The chemical solution of 2mM EDTA (pH 11) used on this particular system and PP 0.2µm membrane showed a sequential cleaning efficiency of 98%, 96%, and 93% recovery of permeate flux that was declined due to wastewater effluent. These conclusions have significant implementations for mitigating fouling of DCMD membranes in wastewater reuse applications.

Future studies could follow a wide variety of paths forward. Different cleaning solutions for removing the wastewater effluent membrane fouling could be examined. Effects of

different levels of EDTA cleaning solution concentration and pH could be investigated. Different membrane types and pore sizes could be used with similar or different cleaning solutions. A similar membrane cleaning process could be used on a DCMD hollow fiber membrane module to offer more surface area. Waste grade heat operation could be studied. A larger scale system could be implemented to run independently long term. The possibilities are endless.

References

1. Alkhudhiri, A., N. Darwish and N. Hilal (2012). "Membrane distillation: A comprehensive review." Desalination: 2.

2. Alklaibi, A. and N. Lior (2005). "Transport analysis of air-gap membrane distillation." Journal of Membrane Science **255**(1-2): 239-253.

3. Amali, A. E., S. Bouguecha and M. Maalej (2004). "Experimental Study of air gap and direct contact membrane distillation configurations: application to geothermal and seawater desalination." Desalination **168**(357).

4. Ang, W. S., S. Lee and M. Elimelech (2006). "Chemical and physical aspects of cleaning of organic-fouled reverse osmosis membranes." Journal of Membrane Science **272**(1-2): 198-210.

5. Ang, W. S., A. Tiraferri, K. L. Chen and M. Elimelech (2011). "Fouling and cleaning of RO membranes fouled by mixtures of organic foulants simulating wastewater effluent." Journal of Membrane Science **376**(1-2): 196-206.

6. Ang, W. S., N. Y. Yip, A. Tiraferri and M. Elimelech (2011). "Chemical cleaning of RO membranes fouled by wastewater effluent: Achieving higher efficiency with dual-step cleaning." Journal of Membrane Science **382**(1-2): 100-106.

7. Banat, F. A. (1994). Membrane Distillation For Desalination And Removal Of Volatile Organic Compounds From Water. Doctor of Philosophy, McGill University.

8. Brown, K. D. (2004). "Pharmaceutically Active Compounds in Residential and Hospital Effluent, Municipal Wastewater, and the Rio Grande in Albuquerque, New Mexico."

9. Cath, T. (2014). "Enhanced Direct Contact Membrane Distillation."

10. Cath, T. Y., V. D. Adams and A. E. Childress (2004). "Experimental study of desalination using direct contact membrane distillation: a new approach to flux enhancement." Journal of Membrane Science **228**(1): 5-16.

11. El-Abbassi, A., H. Kiai, A. Hafidi, M. C. García-Payo and M. Khayet (2012). "Treatment of olive mill wastewater by membrane distillation using polytetrafluoroethylene membranes." Separation and Purification Technology **98**: 55-61.

12. El-Bourawi, M. S., Z. Ding, R. Ma and M. Khayet (2006). "A framework for better understanding membrane distillation separation process." Journal of Membrane Science **285**(1-2): 4-29.

13. Essalhi, M. and M. Khayet (2012). "Surface segregation of fluorinated modifying macromolecule for hydrophobic/hydrophilic membrane preparation and application in air gap and direct contact membrane distillation." Journal of Membrane Science **417-418**: 163-173.

14. Farias, E. L., K. J. Howe and B. M. Thomson (2014). "Effect of membrane bioreactor solids retention time on reverse osmosis membrane fouling for wastewater reuse." Water Res **49**: 53-61.

15. Fujioka, T., S. J. Khan, Y. Poussade, J. E. Drewes and L. D. Nghiem (2012). "N-nitrosamine removal by reverse osmosis for indirect potable water reuse – A critical review based on observations from laboratory-, pilot- and full-scale studies." Separation and Purification Technology **98**: 503-515.

16. Godino, P., L. Pena and J. I. Mengual (1996). "Membrane Distillation: theory and experiments." Journal of Membrane Science **121**: 83-93.

17. Gryta, M. (2005). "Long-term performance of membrane distillation process." Journal of Membrane Science **265**(1-2): 153-159.

18. Gryta, M. (2007). "Influence of polypropylene membrane surface porosity on the performance of membrane distillation process." Journal of Membrane Science **287**(1): 67-78.

19. Gryta, M. (2008). "Fouling in direct contact membrane distillation process." Journal of Membrane Science **325**(1): 383-394.

20. Gryta, M., M. Tomaszewska and K. Karakulski (2006). "Wastewater treatment by membrane distillation." Desalination **198**(1-3): 67-73.

21. Hendren, Z. (2011). "Novel ceramic membranes for membrane distillation: Surface Modification, Performance Comparison with PTFE Membranes, and Treatment of Municipal Wastewater."

22. Holman, S. R. O., Kurt N. (2007). "An Evaluation of Fouling Potential and Methods to Control Fouling in Microfiltration Membranes for Secondary Wastewater Effluent." Water Environment Federation: 6417-6444.

23. Kerry J. Howe, A. Marwah, K.-P. Chiu and S. S. Adham (2006). "Coagulation and membrane fouling." Environ. Sci. Technology **40**: 7908-7913.

24. Khayet, M. (2011). "Membranes and theoretical modeling of membrane distillation: A review." Advances in Colloid and Interface Science **164**: 56-88.

25. Kim, A. S. (2014). "Cylindrical cell model for direct contact membrane distillation (DCMD) of densely packed hollow fibers." Journal of Membrane Science **455**: 168-186.

26. Lawson, K. W. and D. R. Lloyd (1997). "Membrane distillation." Journal of Membrane Science **124**(1): 1-25.

27. Lee, C., K. Howe and B. Thomson (2009). State of Knowledge of Pharmaceutical, Personal Care Product, and Endocrine Disrupting Compound Removal during Municipal Wastewater Treatment.

28. Lee, C. O., K. J. Howe and B. M. Thomson (2012). "Ozone and biofiltration as an alternative to reverse osmosis for removing PPCPs and micropollutants from treated wastewater." Water Res **46**(4): 1005-1014.

29. Madaeni, S. S. and S. Samieirad (2010). "Chemical cleaning of reverse osmosis membrane fouled by wastewater." Desalination **257**(1-3): 80-86.

30. Martinez-Diez, L., F. J. F.J. Florido-Diaz and M. I. Vasquez-Gonzalez (1999). "Study of evaporation effects in membrane distillation." Desalination **126**: 193-198.

31. Mitch, W. A. e. a. (2003). "N-Nitrosodimethylamine (NDMA) as a Drinking Water Contaminant: A Review." Environmental Engineering Science **20**(5).

32. Organization, W. H. (2011). Pharmaceuticals in Drinking-water.

33. Phattaranawik, J., R. Jiraratananon, A. G. Fane and C. Halim (2001). "Mass flux enhancement using spacer filled channels in direct contact membrane distillation." Journal of Membrane Science **187**(1–2): 193-201.

34. Plumlee, M. H., M. Lopez-Mesas, A. Heidlberger, K. P. Ishida and M. Reinhard (2008). "N-nitrosodimethylamine (NDMA) removal by reverse osmosis and UV treatment and analysis via LC-MS/MS." Water Res **42**(1-2): 347-355.

35. Steinle-Darling, E., M. Zedda, M. H. Plumlee, H. F. Ridgway and M. Reinhard (2007). "Evaluating the impacts of membrane type, coating, fouling, chemical properties and water chemistry on reverse osmosis rejection of seven nitrosoalklyamines, including NDMA." Water Res **41**(17): 3959-3967.

36. Susanto, H. (2011). "Review: Towards practical implementations of membrane distillation." Chemical Engineering & Processing: Process Intensification **50**: 139-150.

37. Tomaszewska, M. (2000). "Membrane Distillation Examples & Applications in Technology and Environmental Protection." Polish Journal of Environmental Studies **9**: 27-36.

38. Wang, J., D. Qu, M. Tie, H. Ren, X. Peng and Z. Luan (2008). "Effect of coagulation pretreatment on membrane distillation process for desalination of recirculating cooling water." Separation and Purification Technology **64**(1): 108-115.

39. Warsinger, D. M., J. Swaminathan, E. Guillen-Burrieza, H. A. Arafat and J. H. Lienhard V (2015). "Scaling and fouling in membrane distillation for desalination applications: A review." Desalination **356**: 294-313.